Preliminary Report of the KT 86-10 Cruise for the Mikura and Hachijo Basin.

Kantaro FUJIOKA[1], Masataka KINOSHITA[2], Jai-Ho CHOI[3], Keisuke FUSE[4],
Toshitaka GAMO[1], Kouji HASUMOTO[1], Jun-ichiro ISHIBASHI[1], Kazuhide
KOGA[5], Hiroki MIYATA[6], Ei-ichiro NISHIYAMA[1], Keizo SAYANAGI[1],
Kiyoshi SHIMAMURA[7], Kiminori SHITASHIMA[8], Keiichi SUZUKI[6],
Yuichiro TANAKA[4], Hidekazu TOKUYAMA[1]
and Masaharu WATANABE[1]

1) Ocean Research Institute, University of Tokyo
2) Earthquake Research Institute, University of Tokyo
3) Department of Earthsciences, Faculty of Science, Yamagata University
4) Institute of Geology and Paleontology, Tohoku University
5) Department of Earthsciences, Nihon University
6) Department of Earthsciences, Chiba University
7) School of Agriculture, Kyushu Tokai University
8) Faculty of Integrated Arts and Science, Hiroshima University

(Received April 30, 1987)

Abstract

The Mikura Basin and Hachijo Basin lie just beyond the volcanic
front of the Izu-Ogasawara arc-trench system and the existence of
submarine hydrothermal activity is expected. This area was surveyed
during the cruise of KT 86-10 by the R/V Tansei-Maru, Ocean Re-
search Institute, University of Tokyo from the 12th to the 21st of
July, 1986.

A small topographic high west of the Inanbajima which occupies
the central part of the basin was found by a 12 kHz echo sounder as
well as a seismic profiler. The small topographic high consists mostly
of the boulder of volcanic rocks which were recognized later as two
pyroxene andesites by the submersible "Shinkai 2000" of JAMSTEC.
The other parts of the basins are covered by thick volcanogenic and
biogenic materials having bioturbation structures on the surface by
the bottom dwelling organisms. The geologic developments of the
basins viewed from the present observations are as follows: Basement
of the region was cut by the normal faults relating to the initiation
of rifting the northern Izu-Ogasawara backarc area and followed to
subside. Thick volcanic materials covered the basement. Compressional

stress field after the end of the rifting may take place to form fold-ing and fissure eruption of andesitic lava to make small knoll. CTD (Conductivity, Temperature, Depth) measurements across the knoll were carried out and temperature anomalies were found near the knoll. The temperature and salinity relationship observed along the knoll gives negative possibility to support the existence of present-day hydrothermal activity. Multichannel seismic profiler data show the existence of a low velocity part, which may possibly be a magma chamber, about 1.5 km beneath the Mikura Basin. All the other data support the existence of hydrothermal activity in the basins. However, it will be necessary to have more elaborate surveys of this area in future studies.

CONTENTS

1. Introduction

The Mikura Basin is square in shape and lies southwest of Mikurajima and northwest of the Hachijojima as shown in Fig. 1. Both islands occupy the volcanic front of the northern Izu-Ogasawara Arc and are composed mostly of Quaternary andesites and basalts (ISSHIKI, 1959, 1980). The Inanbajima, which also consists of two pyroxene andesites, occupies just the central part of the Mikura Basin and stands 74 m above the sea (ISSHIKI, 1980). The Hachijo Basin is rectangular in shape and lies west of the Hachijojima. The mean water depth of the Mikura Basin is about 1,800 m and the Hachijo Basin about 1,200 m. The two basins are morpho- logically separated by the topographic high called the Hachijo Nishino-se. The two basins are quite important for understanding present-day sub- marine hydrothermal activity, being expected to take place at the northern portion of the Izu-Ogasawara arc-trench system, because the two basins lie just beyond the volcanic front of the area. FUJIOKA (1983) first pointed out the possibility of the existence of the present-day hydrothermal ore deposits along the back arc side of the Izu-Ogasawara arc. He demon- strated that the northeast Japan arc in the Nishikurosawa age was quite similar to that of the present Izu-Ogasawara arc-trench system and
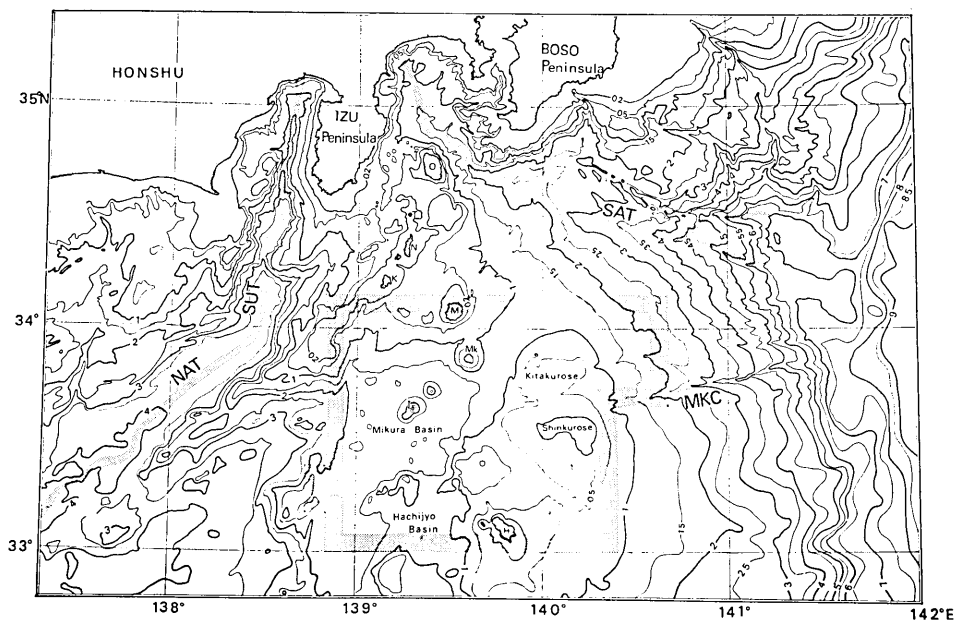

Fig. 1. Index map of the surveyed area during the KT 86-10 cruise. The hatched area indicates surveyed area shown in Fig. 5.

discussed the tectonic setting for the formation of the Kuroko deposits (massive sulfide ore deposits) being similar to that of the present Izu-Ogasawara arc as well.

TAMAKI *et al.* (1981) named the topographic depressions described by ONODERA and MUKAI (1976) which lie just beyond the volcanic front of the Izu-Ogasawara arc as "Back Arc Depression".

They suggested that these depressions are formed by the rifting of

Table 1.   Station survey log

Sampling No.	Area	Latitude (North)	Longitude (East)	Water Depth (m)	Device
G-1	1	33°08.1′	139°24.3′	1294	Okean
PC-1	1	33°08.0′	139°24.4	1290	Piston
PC-1′	1	33°07.9	139°24.5	1294	Piston
HF-1	1	33°08.0	139°23.5	1289	Heat Flow
D-1	2	33°07.8	139°30.4	1144	Dredger
C-1	2	33°08.0	139°30.0	1240	Camera
G-2	3	33°37.2	139°08.6	1860	Okean
PG-2	3	33°36.9	139°08.2	1879	Piston
PG-2′	3	33°36.9	139°08.5	1901	Piston
PC-2″	3	33°37.9	139°09.2	1872	Piston
HF-2	3	33°36.9	139°08.3	1885	Heat Flow
PC-3	4	33°48.2	140°38.3	1867	Piston
HF-3	4	33°48.0	140°37.9	1885	Heat Flow
G-3	5	33°40.3	140°30.0	1693	Okean
G-4	6	33°43.3	140°09.4	533	Okean
G-5	6	33°47.9	140°11.0	344	Okean
G-6	6	33°48.0	140°08.6	321	Okean
G-6′	6	33°47.8	140°08.7	321	Okean
CTD-1	3	33°37.1	139°09.5	1910	CTD+W.S.
CTD-2	3	33°36.7	139°08.2	1908	CTD+W.S.
CTD-3	3	33°38.6	139°10.0	1870	CTD+W.S.
CTD-3-1	3	33°38.4	139°10.2	1830	CTD+W.S.
CTD-4	3	33°38.3	139°07.6	1854	CTD+W.S.
C-2	3	33°38.4	139°08.1	1887	Camera
PC-4	3	33°38.4	139°10.6	1862	Piston
HF-4	3	33°37.6	139°09.5	1891	Heat Flow
C-3	3	33°38.3	139°09.7	1873	Camera
D-2	7	33°30.8	140°03.4	167	Dredger
D-2′	7	33°30.8	140°03.5	166	Dredger
G-7	7	33°33.9	140°08.0	180	Okean
D-3	7	33°33.8	140°08.1	180	Dredger
D-4	7	33°33.9	140°08.6	184	Dredger

1 : Hachijo Basin   2 : Kenken Seamount   3 : Mikura Basin   4 : Izu-Ogasawara Forearc

the backarc during the Quaternary period. Later, TAMAKI (1984) discussed the mechanism of the opening of these backarc depressions. FUJIOKA (1983) recognized the situation of the backarc depressions as equivalent to the depositional environment of the Kuroko deposits emplaced during 15Ma in the northeast Japan Arc. UYEDA (1983) supported Fujioka's idea and stated that the Izu-Ogasawara arc as well as the Okinawa Trough are the field of the present-day hydrothermal ore deposits, which is deduced from

during KT 86-10 cruise.

Date M./D.	Time, Start	Time, Hlt Bottom	Wire Length	Time, Leave Bottom	Time, Finish	Sample Recoverd
7/13	10 : 08	10 : 32	1337	10 : 32	10 : 47	○
7/13	11 : 48	12 : 15	1332	12 : 15	13 : 44	×
7/13	13 : 50	14 : 13	1306	14 : 13	14 : 31	○
7/13	15 : 02				17 : 40	—
7/13	18 : 24	18 : 51	1274	19 : 40	19 : 53	○
7/13	20 : 17	20 : 43		21 : 57	22 : 14	—
7/14	11 : 08	11 : 33	1892	11 : 33	11 : 55	○
7/14	12 : 15	12 : 48	—	12 : 48	13 : 12	×
7/14	13 : 12	13 : 41	—	13 : 41	14 : 05	×
7/14	14 : 37	15 : 15	1902	15 : 15	15 : 50	○
7/14	16 : 23				19 : 08	—
7/15	10 : 00	10 : 33	1886	10 : 33	11 : 05	○
7/15	11 : 21				14 : 13	—
7/15	16 : 20	16 : 50	1718	16 : 50	17 : 09	○
7/15	19 : 50	20 : 02	557	20 : 02	20 : 10	○
7/15	21 : 12	21 : 21	336	21 : 21	21 : 28	○
7/15	21 : 58	22 : 06	331	22 : 06	22 : 12	○
7/15	22 : 18	22 : 24	332	22 : 24	22 : 24	○
7/19	13 : 13				16 : 08	—
7/19	16 : 25				19 : 19	—
7/19	20 : 56					—
7/19	21 : 37					—
7/20	02 : 24					—
7/20	06 : 02	06 : 42		07 : 57	08 : 25	—
7/20	09 : 02	09 : 43	1874	09 : 43	10 : 15	○
7/20	10·· 45				13 : 25	—
7/20	13 : 47	14 : 26		15 : 42	16 : 08	—
7/20	21 : 00	21 : 05	170	21 : 11	21 : 15	○
7/20	21 : 16	21 : 20	172	21 : 38	21 : 47	○
7/20	22 : 22	22 : 28	184	22 : 28	22 : 35	○
7/20	22 : 38	22 : 41	193	22 : 57	23 : 03	○
7/20	23 : 12	23 : 17	193	23 : 34	23 : 40	○

5: Mikura Canyon 6 Kitakuros Bank 7: Shinkurose Bank

his classification of the arc-trench system in terms of Chilean and Mariana
type subduction modes.   Under such conditions, a five year project of the
Geological Survey of Japan for the hydrothermal ore deposits started in
1984 for the target area of the Izu-Ogasawara arc-trench system.

Research cruise, KT 86-10 (DELP 1986 cruise) of the Ocean Research
Institute, University of Tokyo was carried out using the R/V Tansei-
Maru (460 tons) from the 12 th to the 21 st of July, 1986 in the area of
the Mikura and Hachijo Basins as shown in Figs. 1 and 2 and Table 1.   The
two basins are thought to be the northern extension of the backarc
depressions and the area expected to have present-day hydrothermal activity
along the depression.   On this cruise, therefore, CTD with seawater
samplers were carried out for the detection of the hydrothermal activity
in addition to ordinary studies such as topographic, seismic survey,
sampling of sediments and rocks and heat flow measurements.   The sur-
veyed area covers both the Mikura and Hachijo Basins and the easternmost
part of the Shikoku Basin as well as the Kurose Bank chain (HONZA and
TAMAKI, 1985).   The results are still immature for each item.   However,
we intend to describe here the preliminary data for the cruise because of
their suitability to future study.

2.   Topography

The northern part of the Izu-Ogasawara arc-trench system is close to
Tokyo, but few precise geological surveys have been carried out so far.
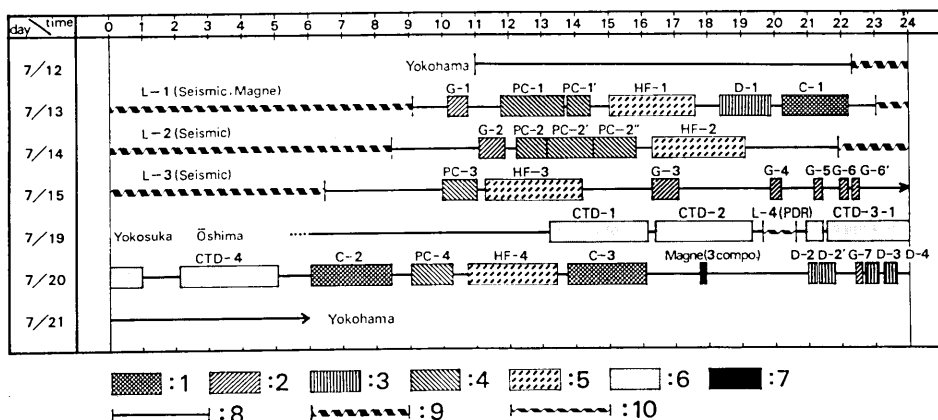

Fig. 2.   Working diary of the KT 86-10 cruise.   1: deep sea camera, 2: "OKEAN"
grab sampling, 3: dredge sampling, 4: piston core sampling, 5: heat flow measure-
ment, 6: CTD with water sampling, 7: three components geomagnetic field measure-
ments, 8: steaming, 9: multichannel seismic profiling, 10: Special line of 12 kHz
echo-sounder.

The HYDROGRAPHIC OFFICE, MARITIME SAFETY AGENCY carried out a topographic survey of this area and published several topographic maps on various scales (1980a, 1980b, 1982), As for the southern area from the Hachijojima, few reliable topographic maps are available. A multi-narrow beam (Sea beam) survey was carried out for only several single lines across the Izu-Ogasawara arc as a transit from the Suruga to the Sagami Boxes during the KAIKO Project Phase I, Leg II (FUJIOKA and NAKAMURA, 1984MS).

Therefore, in this article, we will describe the morphologic features of the area using the topographic maps published by HYDROGRAPHIC OFFICE, MARITIME SAFETY AGENCY, (1980a, 1980b, 1982) and the results of the surveys done by the Hydrographic Office (SAKURAI and OGAWA, 1982) and by the GEOLOGICAL SURVEY OF JAPAN (1985) as well as the morphologic features obtained during the KT 86-10 cruise.

2-1. Topographic overview

The topography of the surveyed area is shown in Figs. 1 and 5 which was traced from the bathymetric map for scales 1:1,000,000 and 1:200,000. The Izu-Ogasawara arc-trench system is bounded by the Izu-Ogasawara trench in the eastern margin, which continues about 800 km from north to south. The water depth of the trench becomes shallower around the Ogasawara Plateau because of the collision and subduction between the Izu-Ogasawara arc-trench system and the Ogasawara Plateau. In the northern part of Hachijojima the width of the arc-trench system becomes narrower toward the Izu Peninsula than the other portion. The volcanic front of the arc-trench system runs along the lines connecting the Oshima, Miyakejima and Hachijojima and the Quaternary basalts and andesites are yielded by the volcanic activity taking place along these lines. Across the volcanic front lie Ohmurodashi, Niijima and Kozushima which are composed of Quaternary rhyolitic rocks and the topographic high consisting of these acidic rocks extends as far as the Zenisu Ridge in the Shikoku Basin.

The drainage system is largely separated by the eastern and western volcanic fronts. The large canyon transporting the sediments to the east is the Minami Mikura Canyon which was thought to be a consequent valley on the Philippine Sea Plate (FUJIOKA, 1985, TAKEUCHI and FUJIOKA, 1985). This canyon may be a tectonic line caused by the bending of the Philippine Sea Plate being subducted under central Japan (FUJIOKA, 1985). On the other hand, downstream to the west of the arc-trench system are the Zenisu and Iro canyons, which were thought by ISHIBASHI (1984) to be the tectonic "Izu Toho Line".

The Mikura Basin is a square shaped basin having various sized sea-
mounts and volcanic islands, among which Inanbajima occupies the center
of the basin standing 74 m above sea level. Inanbajima is quite small if
we look only at the subaerial part, but the area circled by the 1,500 m
contour line is as large as 15 km in the long axis. Northeast of the
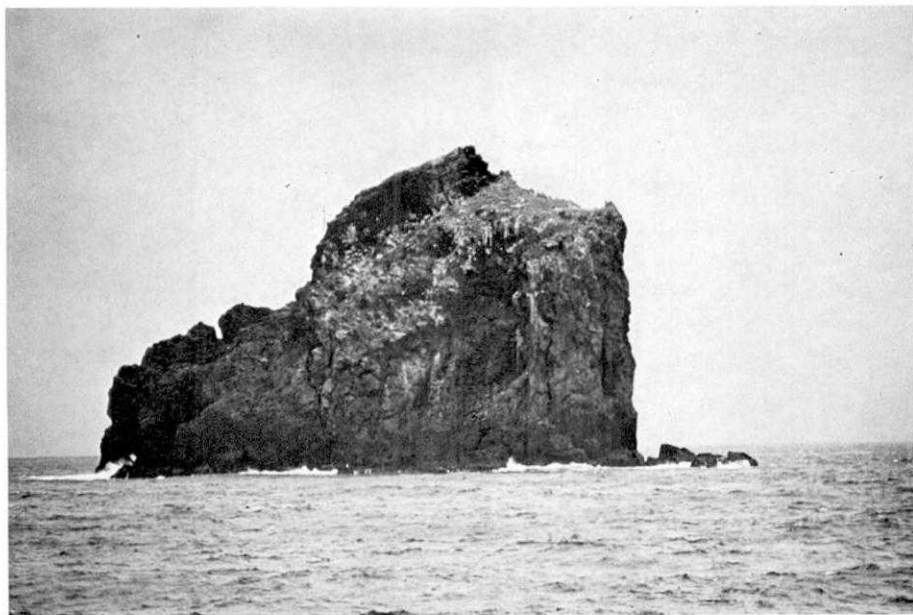Inanbajima, is the Mikura Seamount which forms a twin volcano, and
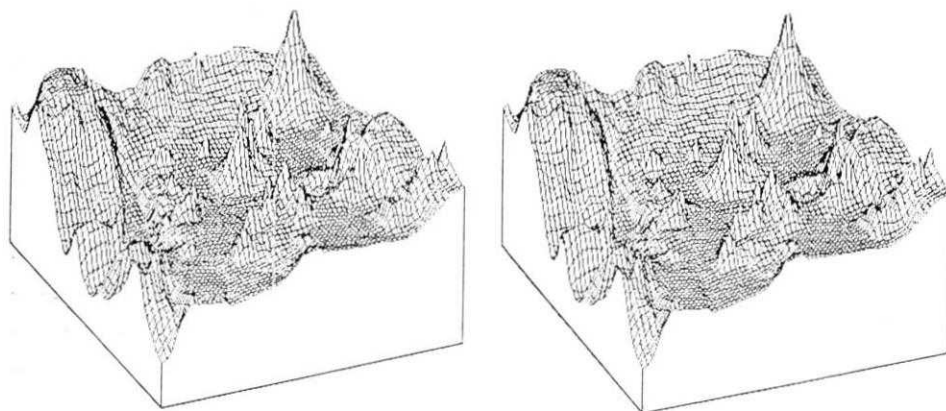

Fig. 3. Photograph of Inanbajima.

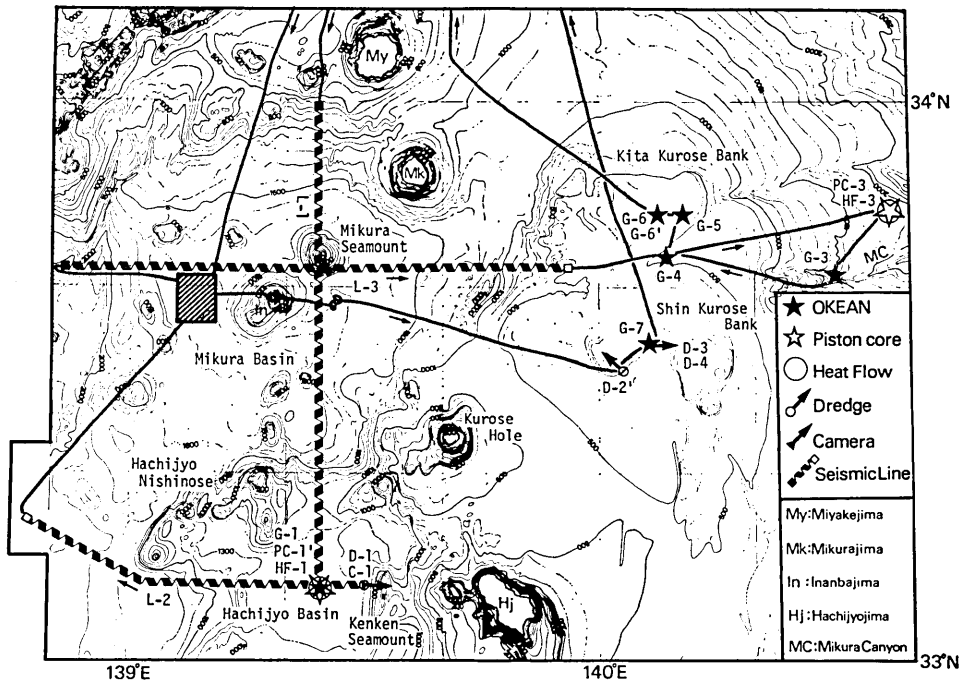Fig. 4. Stereographic whale's eyes view of the Mikura Basin and its adjacent area.

Fig. 5. Ship's track lines and surveyed area. The hatched square indicates the area shown in Figs. 6 and Fig. 7.

seems to continus northeast to the Mikurajima making a volcanic line trending northeast to southwest.

There is some drainage into the basin as is clearly seen in Figs. 1 and 5. Therefore, small amounts of terrigenous material may be expected to be transported to this basin. The water depth of the basin becomes deeper towards the center but the southwestern portion of the basin is open to the south. The deepest portion of the basin is located south of the Inanbajima being slightly over 2,000 m.

The Hachijo Basin is rectangular in shape and the mean water depth is less than of the Mikura Basin. The two basins are separated morphologically by the Hachijo Nishinose. The Hachijo Basin has little drainage into the basin and terrigenous material is thought to be scanty.

The Kuroshio, one of the largest warm streams, runs along the Japanese Islands from near the Philippines and cuts across the Izu-Ogasawara arc-trench system. The center of the stream flows between the Mikurajima and Hachijojima frequently depending on the global circulation of air and water. The thickness of the stream is about 500 m in the central portion of the stream, therefore the marine area shallower

than 500 m may be effected by the sedimentation of the materials transported to the basin and the distribution of temperature and salinity of seawater may be greatly changed by the stream.   The eastern edge of the Mikura Basin seems to be cut by the fault running south of the Mikurajima and it also seems that the western margin of the basin is cut by conspicuous faults.   These features are well reflected on the east-west cross section of the seismic profile line.   Therefore, the two basins are thought to be a kind of volcano-tectonic depression fault bounded on the both sides of the basin.   The backarc depressions become deeper toward the south from Hachijojima, Sumisujima (Smith), Torishima and Nishinoshima.   When we look at the Mikura and Hachijo Basins whose water depths are less than 2,000 m and have depression structures, these two basins should be called the Mikura and the Hachijo-north depressions, respectively.   The latter is an anomalously shallow backarc depression in this area.

In the Mikura Basin, various sizes of circular topographic highs surround the Inanbajima.   They may be kind of seamounts or knolls.

Between Mikurajima and Hachijojima, there is a large depression called the Kurose Hole which may be caldera in shape and large pumice fragments were recovered by dredge hauls (FUJIOKA *et al.*, 1979).

The Shinkurose Bank lies east of the Kurose Hole.   Topographically the Shinkurose Bank is divided into three portions: namely, Kitakurose, Nakanokurose and Shinkurose.   The Shinkurose Bank is the deepest, having about a 400 m water depth, the Nakanokurose 300 m and the less than 200 m Shinkurose.   All the banks are covered with limestone and have flat surfaces possibly being eroded by waves.   The difference in the water depths of the three banks may be caused by the different distances from the fault movement.

According to the interpretation of the seismic profile data across the Kurose Bank from both north to south and east to west, the Kurose Bank has a flat surface tilting gently to the northeast as a whole.   This evidence was interpreted to mean that the bending of the Philippine Sea Plate carrying the Kurose Bank on its surface caused the tilting of the Kurose Bank during the subduction of the Philippine Sea Plate under the Sagami Trough (FUJIOKA *et al.*, 1984).

2-2.   Precise topographic study by the 12 kHz echo sounder

During the cruise, bathymetric survey using the 12 kHz echo sounder (Precise Depth Recorder; PDR) was carried out along all ship's lanes.   In this chapter, descriptions of the morphologic features by the PDR data
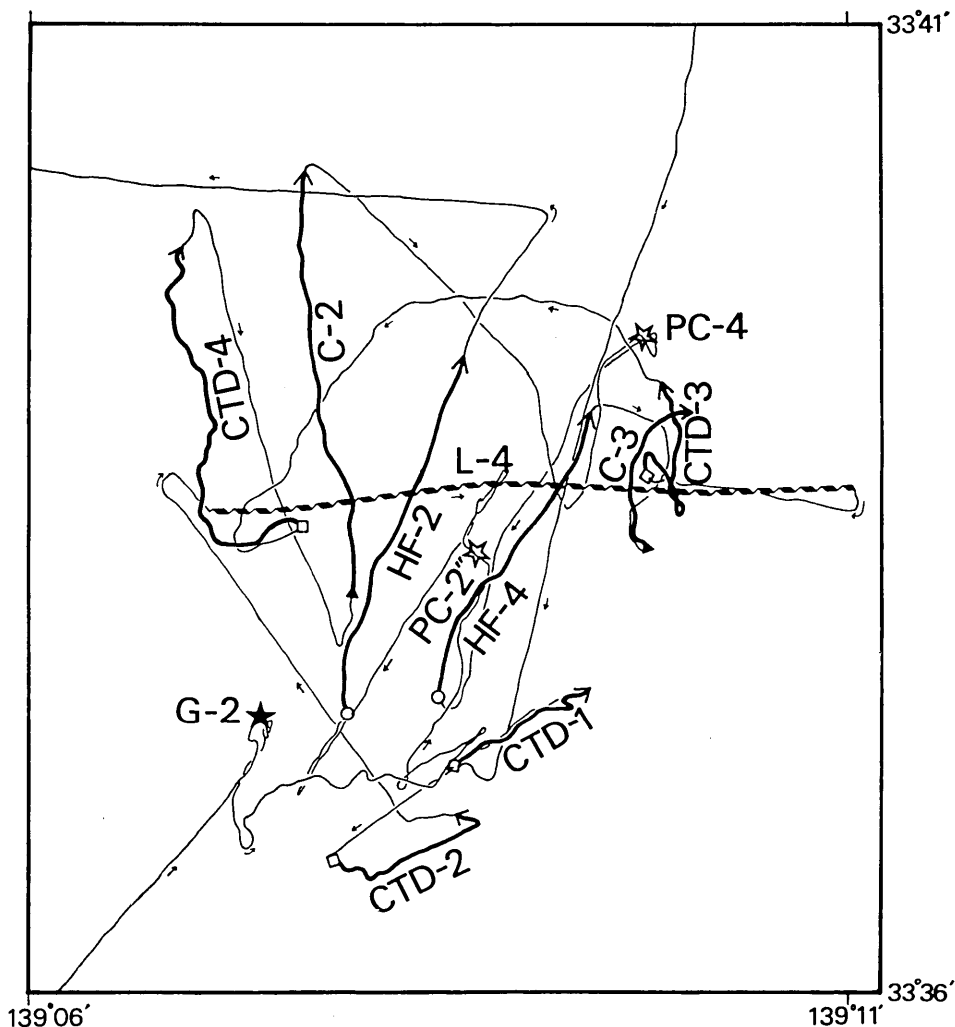
Fig. 6. The detailed ship's tracks and positions of station surveys within the hatched
area in Fig. 5.

from this area are presented.   The six topographic sections were taken
from the area for the precise analysis of the small knoll.   Fig. 7 shows
the precise ship's lanes crossing the small knoll and the thick lines (A–A′
to F–F′) in this figure indicate the range of the topographic cross sections
in the following figures (Fig. 7a to Fig. 7f).   On these sections, the dis-
tance and the dip of slopes were not the same, because the ship's speed
frequently changed so much owing to the waves and winds during the
topographic survey.   The ship's speeds ranged from 5 to 10 knots (kt.)
while sailing from station to station and from 0.2 kt. to 0.5 kt. during the
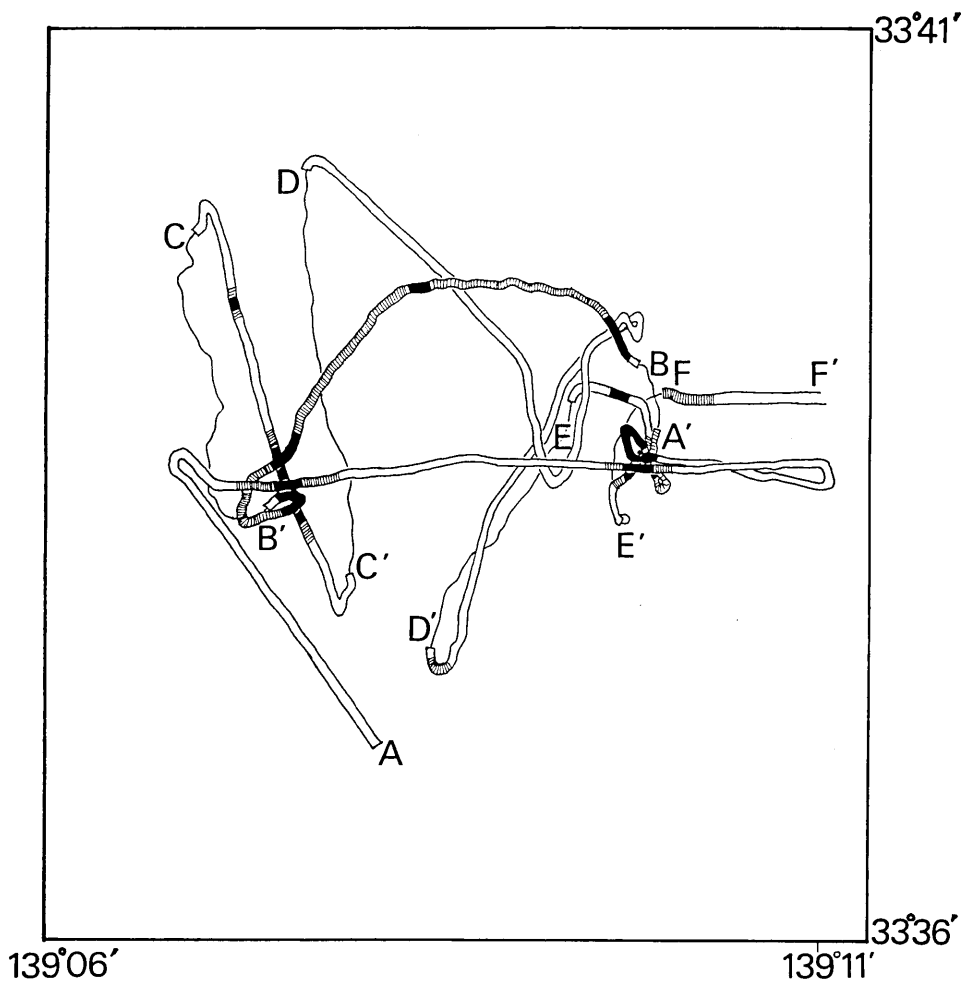
Fig. 7. Index map of the profiling lines with 12 kHz echo-sounder within the hatched
    area in Fig. 5.

station surveys. In Fig. 7, the thick solid lines show the places where
the plume-like features were observed in the topographic cross sections
and the hatched lines show the side echo deduced from the plume-like
topographic highs of line A–A′ to line F–F′. Descriptions on the morpho-
logic features of each line will be presented.

Line A–A′ (Fig. 7a)

    Line L–4 (left half of Fig. 7a) included in A–A′ was obtained for the
reconfirmation of the diagnostic feature of the acoustic plume-like re-
flection patterns which were observed during the cruise of the Geological
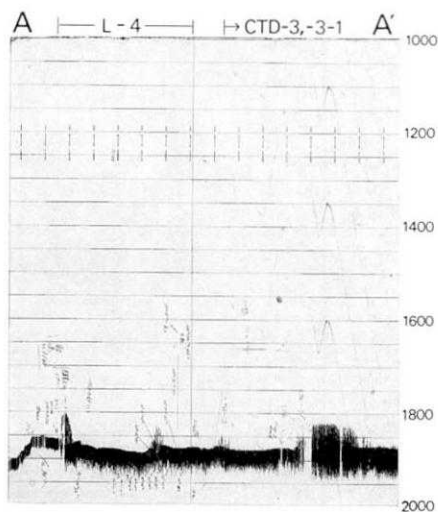Survey of Japan (due to hydrothermal activity) in the western part of the
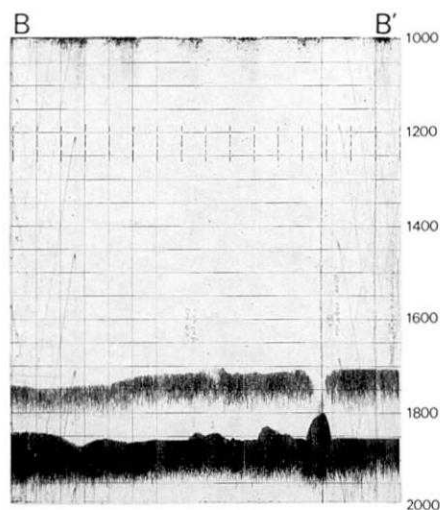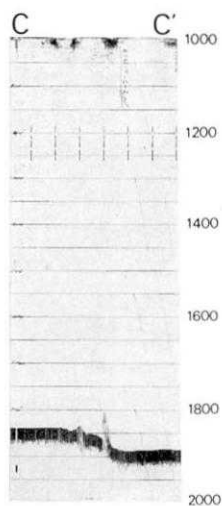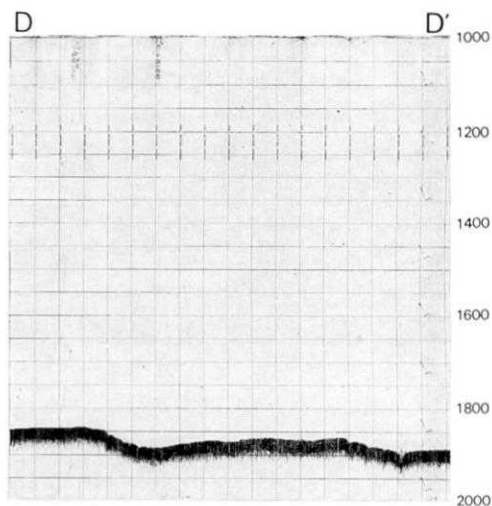
Fig. 7a.

Fig. 7b.

Fig. 7c.

Fig. 7d.

Mikura Basin. The survey was carried out with the ship's speed of about 3.1 kt. on line L-4. There were two conspicuous plumes on the west and east margins of this line. The depth of the peak of the former plume was 1,805 m at the summit. The sea floor was displaced by eastward dipping normal faults beneath this plume. The vertical displacement of this fault was estimated from the figure to be about 10 m. There was no echo from the bottom surface just beneath the plume. The depth of the peak of the eastern plume was 1,830 m. The sea floor was cut by normal
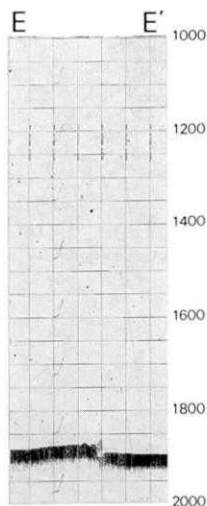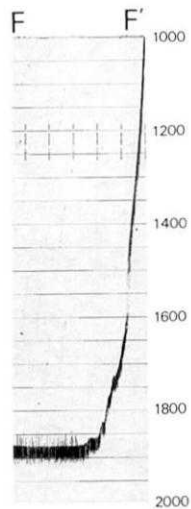
Fig. 7e.

Fig. 7f.

faults with westward dippings beneath the plume. The vertical displacement by the faults was estimated to be about five meters. The right half of section A-A' in Fig. 7a was the topographic record of the station surveys CTD-3 and CTD-3-1. The ship's course was changed after the line, L-4 measurement then, the plume from the right hand side of the figure was the northern extension of the east plume of L-4.

Line B-B' (Fig. 7b)

This topograhic cross section was obtained while sailing from sites CTD-3-1 and CTD-4. Some plumes rise from the sea bottom surface. The two plumes observed in the right side of the figure are the northern and southern extensions of the western plume on line L-4, respectively. The height of the right plume was about 50 m from the sea floor. The records of echo between 1,700 m and 1,750 m were due to multiple reflections.

Line C-C' (Fig. 7c)

The record was taken while sailing from sites CTD-4 and C-2. Two plumes were recognized in the central part of the record. The water depth of the northern plume was 1,835 m at the peak and had about a 10 m height from the bottom surface. The water depth of the southern plume at the peak (right peak in the figure) was 1,805 m. The depth of sea floor changed at this position, that is, the water depth of the north side of the northern plume was 1,865 m whereas the water depth of the

south side was 1,880 m, deeper than that on the north side. The south plume corresponded to the west plume on line L-4.

Line D-D' (Fig. 7d)

In this section two zones of a combination of steep cliffs and benches were recognized. These morphological features were formed by the stepwise development of normal faults. The plume was located at the southern end of this line (right most side). The height of the plume was 20 m from the bottom surface.

Line E-E' (Fig. 7e)

The echo of the plume was recognized on this profile. The depth of the plume was 1,860 m at the peak. The floor was cut by faults at this position. The vertical separation was estimated to be 15 m. This plume corresponded to the eastern plume of line L-4.

Line F-F' (Fig. 7f)

This profile shows the topographic cross section from the western part of the Mikura Basin to the western slope of the Inanbajima. The side echo of the plume was recorded at 1,850 m water depth. Steep cliffs due to some faults were developed at the lower part of the slope, especially at intervals between 1,500 m and 1,600 m in water depth. The cliff was so steep that the reflection of the bottom surface was not clear.

Some acoustic plumes were recognized in the profiles mentioned above, in which the two acoustic plumes under line L-4 were even reconfirmed by the other lines. These plumes showed about a 300 m width and could be tracedm ore than 800 m. The trend of these plumes was estimated to be from NNW to SSW. These acoustic plumes were characterized by the presence of the steep cliff due to normal faults.

2-3. Multichannel reflection survey in the Mikura Basin

The Mikura Basin showed a morphology similar to caldera. A dimension of the Mikura Basin, 60 km × 40 km slightly elongated in a NE-SW direction, was extraordinary huge when compared those of onland calderas (FUJIOKA, 1985). Several seamounts such as Mikurajima, the Mikura Seamount, Inanbajima and unnamed seamounts are aligned in a NE-SW trend in the central portion of the basin. To clarify a subcrustal structure of the Mikura Basin, three multichannel seismic profiles were obtained during the KT 86-10 cruise.
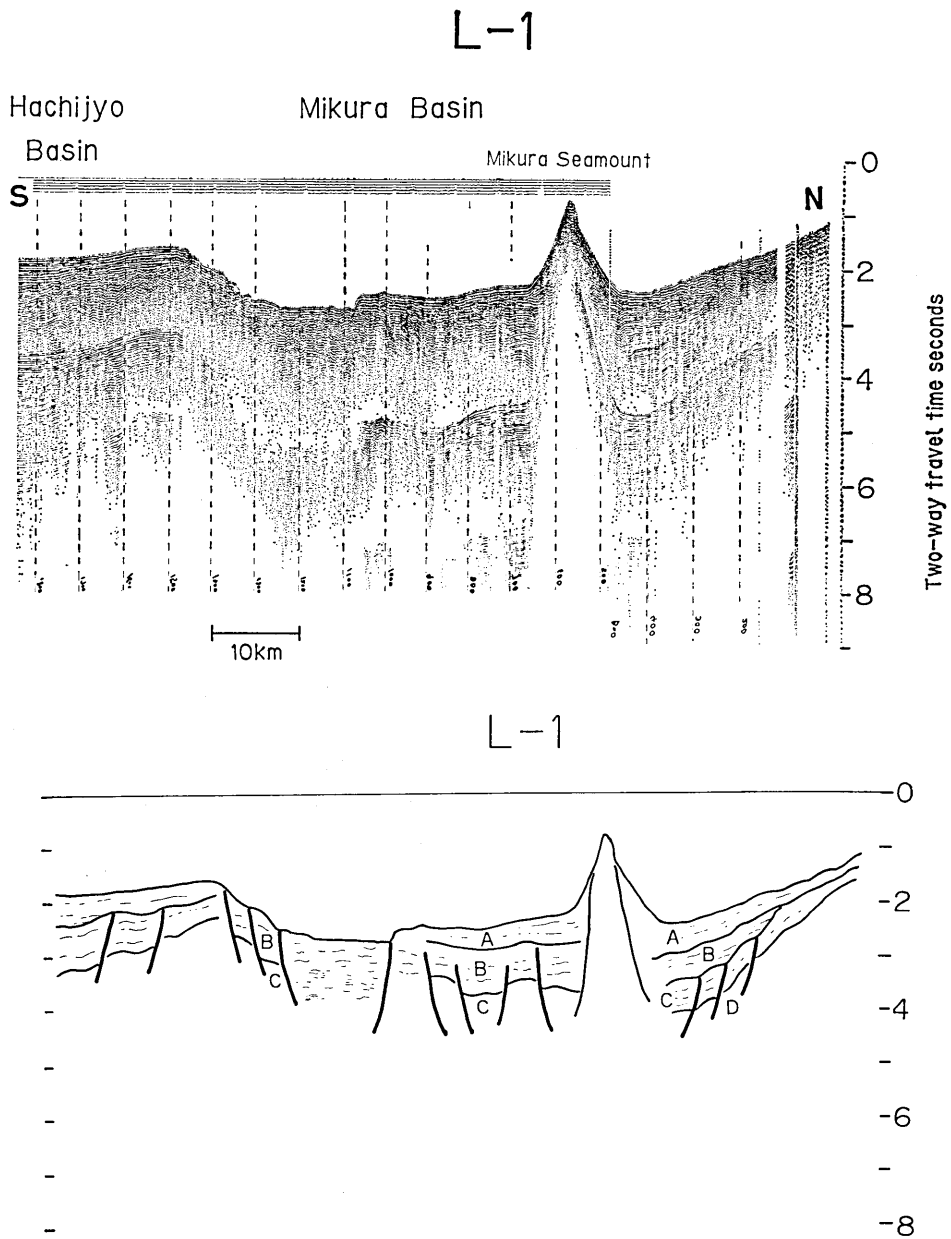
L-1

Hachijyo
Basin

Mikura Basin

Mikura Seamount

S

N

Two-way travel time seconds

10Km

L-1

Fig. 8a.

(a)-U Seismic reflection profile of line L-1.
(a)-L Sketch of the interpretation of line L-1.

L-2

NW   SE →|← W   Hachijyo   E
                                Basin

Two-way travel time seconds

-0
-
-2
-
-4
-
-6
-
-8

10km

L-2

Upper

Middle

Lower

0
-
-2
-
-4
-
-6
-
-8

Fig. 8b.

(b)-U   Seismic reflection profile of line L-2.
(b)-L   Sketch of the interpretation of line L-2.

L-3

Mikura Basin

W   E

Mikura
Inanba   Seamount
Shima

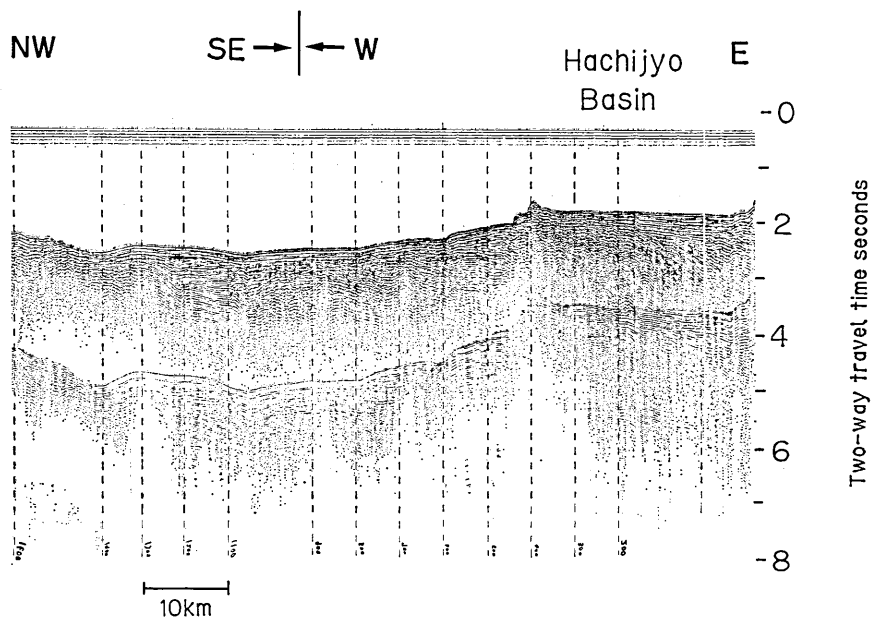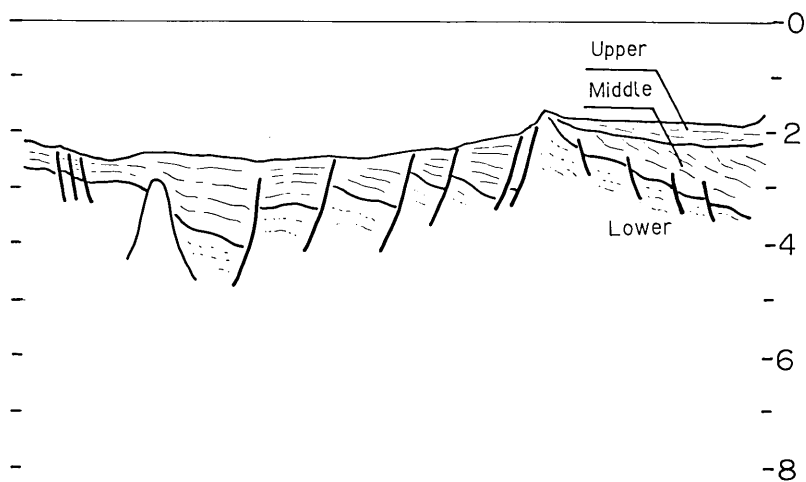Two-way travel time seconds
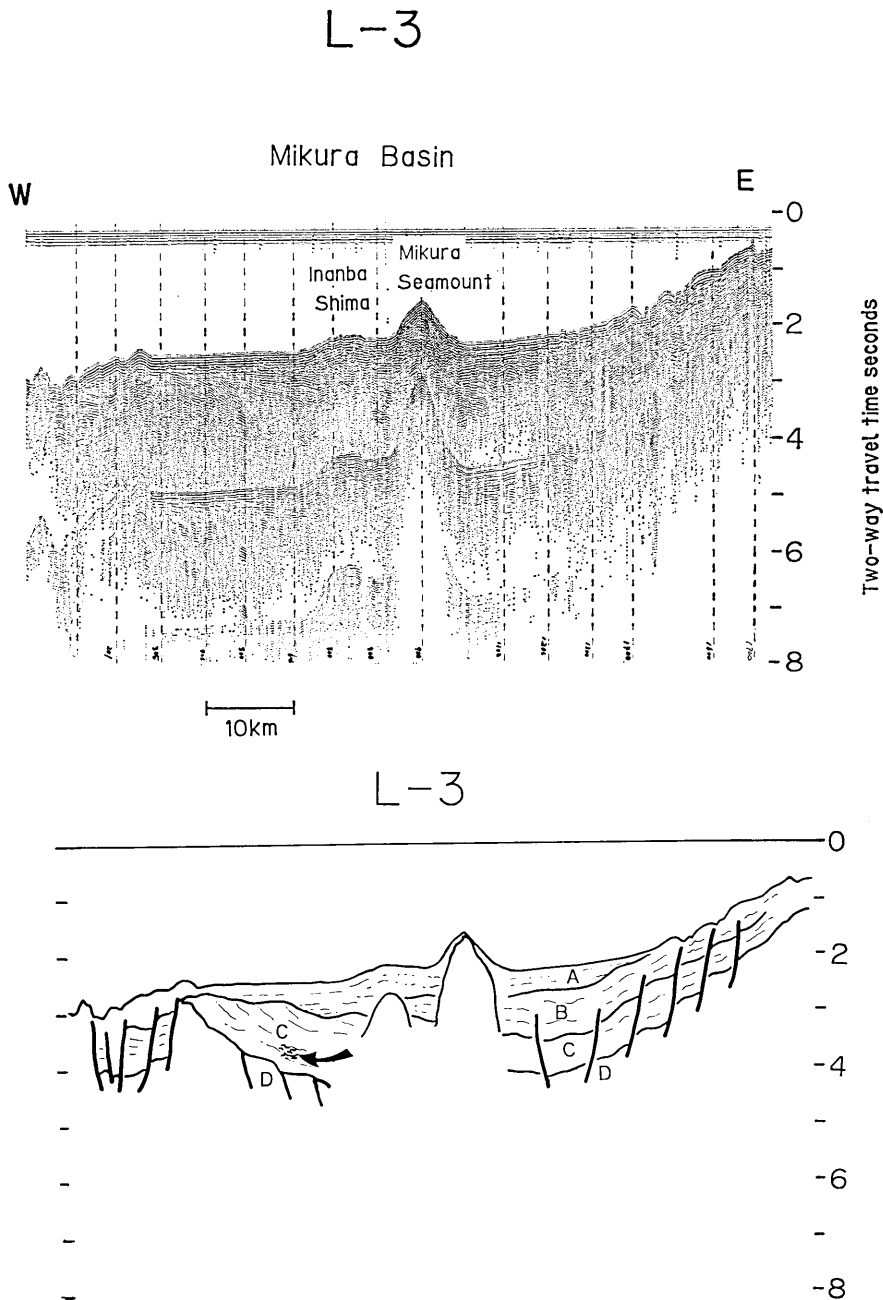
10km

L-3

A

B

C

C

D

D

Fig. 8c.

(c)-U Seismic reflection profile of line L-3.
(c)-L Sketch of the interpretation of line L-3.

Fig. 8. Multichannel seismic reflection profiles and those interpreted
in the Mikura and Hachijo Basins.

2-3-1. Description of each profile

Line L-1

   The line L-1 ran north to south across the Mikura Basin and the Hachijo Basin. The acoustic stratigraphic sequence in the Mikura Basin was identified with units A, B, C and D in descending stratigraphic order (Fig. 8a). Many normal faults were observed in the Mikura Basin, especially in the sequences below unit B. North of the Mikura Seamount unit D, acoustic basement, stepped down successively toward the center of the basin by normal faults and unit B terminated up dip toward the north progressively against the surface of unit C. Unit C was traceable as far as the northern wall of the basin. South of the Mikura Seamount unit D could not be identified. A small caldera-like depression bounded by active normal faults was located at the southern margin of the basin. The fact that acoustic units were not identified beneath the small caldera suggests that the caldera was a recently origin.

Line L-2

   Line L-2 is composed of two sub-lines. An eastern sub-line crossed the central part of the Hachijo Basin in a E-W direction, and an eastern subline parted from the Hachijo Basin in a NW-SE direction.
   Three acoustic units were identified in the basin those are the upper, middle, and lower units (Fig. 8b). Many normal faults were observed in both the middle and lower units of the Hachijo Basin. The lower unit of the basin stepped down progressively toward the east by normal faults. The middle unit terminated at the surface between the middle and upper units. To the west of the Hachijo basin, two acoustic units were identified with many normal faults separating the acoustic basement into several blocks. Each block not only showed sliding with neighbors but also rotation.

Line L-3

   Line L-3 passed through the Mikura Basin from west to east. The eastern terminal of the line was located at the southwestern margin of the Kitakurose Bank. As was previously mentioned, four acoustic units were identified (Fig. 8c). Different from the N-S trending of line L-1 this profile does not show onlap relation between the boundary of units B and C. Unit B had its depocenters at the eastern portion of the basin and was traced as far as the southwestern margin of the Kitakurose Bank. These evidences suggested that unit B consists of volcaniclastic sediments transported from east of the Mikura Basin. Depocenter of unit C was located at the western portion of the Mikura Basin. The eastern

migration of depocenter indicated the formation of two small calderas in different ages. This idea was supported by the fact that unit C in the eastern portion was disturbed by many normal faults associated with the formation of a later caldera different from that in the western portion. Unit C was not only traced as far as the southwestern margin of the Kitakurose Bank but also as far as the northern wall of the Mikura Basin. Unit C was interpreted to be of volcaniclastic origin derived from northeast of the Mikura Basin. As was observed from line L-1, unit D stepped down successively toward the center of the basin by normal faults in the eastern and western portions of the Mikura Basin.

2-3-2. Development of the Mikura Basin

It was reported that the back arc depression in the Izu-Ogasawara Ridge was bounded by normal faults whose trend was approximately in a N-S direction (HONZA and TAMAKI, 1985). But the Mikura Basin did not show a N-S elongated trend but a morphology similar to caldera. Two seismic profiles which run across the Mikura Basin from north to south and east to west revealed that the acoustic basement stepped down successively toward the center of the basin by normal faults. This fact strongly lead to the conclusion that the Mikura Basin was derived from caldera after volcanic eruption. But there was a big debate in regard to dimension because the Mikura Basin was extraordinarily huge when compared with onland calderas. A small caldera bounded by active normal faults was observed at the southern margin of the basin from line L-1. Line L-3 also indicates that the depocenters of units B and C are correlated with small calderas formed in different ages. These evidences suggested that the Mikura Basin is composed of several small calderas.

2-3-3. Bright spot in the Mikura Basin

In line L-3, a bright spot was discovered around shot number 500 (Fig. 9). The bright spot was located about 3.5 seconds in two way travel time below sea level. Fig. 10-(A) showed a directly received wave of shot number 495 transmited from a large air gun (approx. 12l). Fig. 10-(B) is a reflected wave of the same shot number in the vicinity of the bright spot. Hatched and blank parts represent positive and negative phases of the waves, respectively. We could identify at least five wave peaks from the direct waves (A, B, C, D, and E) and reflected waves (A', B', C', D', and E'). These wave peaks were generated by bubble oscillation. The first arrival of the direct wave (A) was characterized by the negative phase, however, that of the bright spot (A') indicated the positive phase.

(shot number)

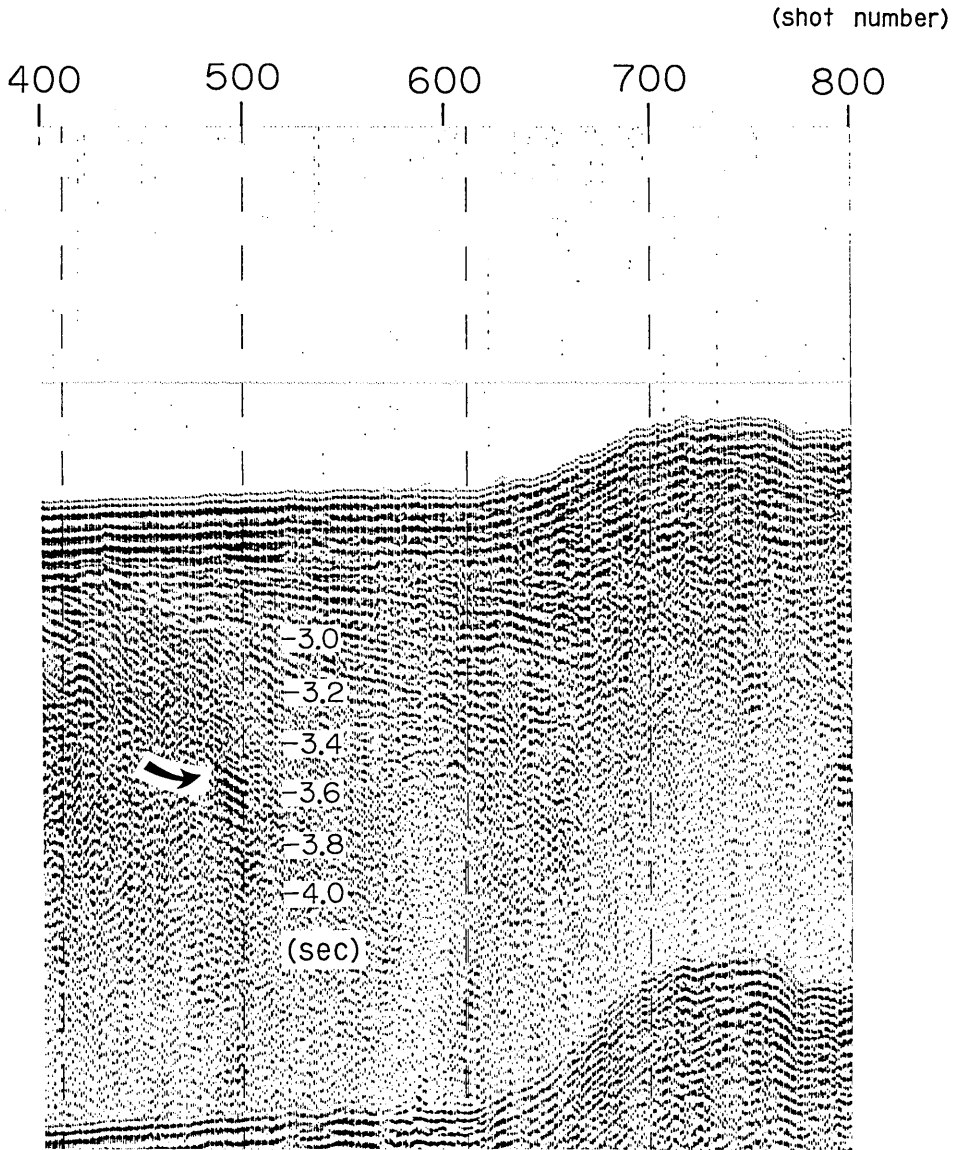400   500   600   700   800

Fig. 9.   Enlarged seismic profile from line L-3.   Arrow indicates the bright spot.

The four subsequent wave peaks also showed good phase reverse correlations
between the direct wave and the bright spot, respectively.   There would
be a phase reversal if the incident ray was in the higher impedance
material.   This fact meant that a low velocity zone existed at about 1.1
seconds below the sea bottom.   We interpreted the low velocity zone to
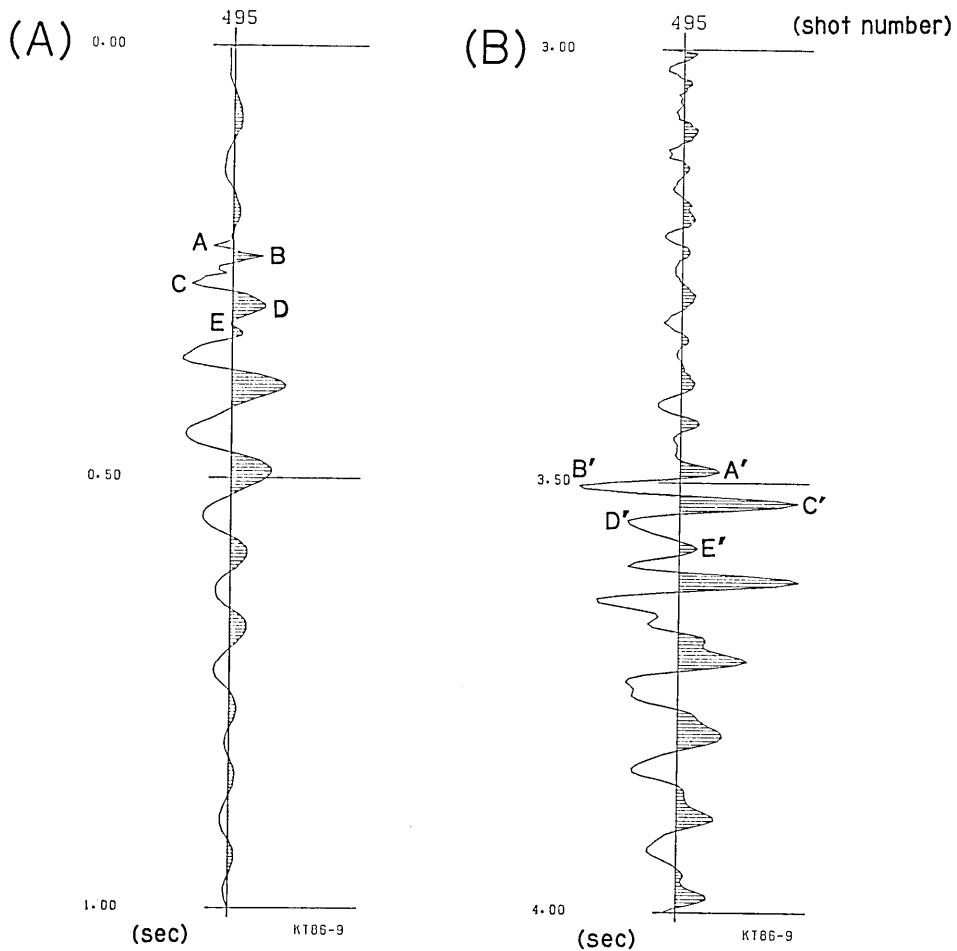be a possible magma reservoir in the caldera, Mikura Basin.

Fig. 10. Comparison between direct signal (A) and
bright spot signal (B) at shot number 495.

3. Sediments and rocks

Sediments and rock samples were collected from the Hachijo Basin,
the Kenkenyama Seamount, the Mikura Basin, the Izu-Ogasawara forearc
region (east of the Kurose Bank), the Shinkurose Bank and the Kitakurose
Bank using a piston corer, a "OKEAN" type grab sampler and a dredger.
Observation of the deep sea bottom was also carried out by using the deep
sea camera system.

The sampled sites, their water depths and kinds of devices used are
listed in Table 1. The purposes of the sampling at each site are explained
below.

In the central part of the Hachijo Basin sediments were taken using the "OKEAN" (G-1) and piston corer (PC-1') in order to know what kind of sediments are transported in the basin. On the western slope of the Kenkenyama Seamount, rocks and surface sediments were taken using the dredge system (D-1) for the purpose of finding out the rocks forming the seamount. A deep sea camera (C-1) was used to take photographs of the surface of the steep slope which may have been caused by faulting.

The Mikura Basin, one of the back arc depressions, was surveyed with the hope of discovering the present hydrothermal activities. Therefore, the samplings were carefully done by using the "OKEAN" (G-2), a piston corer (PC-2″, PC-4) and a deep sea camera (C-2, C-3) wich the aim of making clear whether or not the bottom sediments are affected by hydro-thermal activity and to observe the migration of hot water ejected from the sea floor.

The site east of the Kurose Bank was chosen as the reference site for the biostratigraphic study of warm water species and heat flow measure-ments across the arc-trench system of the Izu-Ogasawara fore arc compare those features with the opposite of the back arc depressions such as the Mikura Basin. Piston core samples (PC-3) were taken from the forearc slope and "OKEAN" grab sample (G-3) was taken from the Mikura Canyon in order to recognize the material transported from the Kurose Bank which shows extremely high positive gravity anomaly in this arc-trench system.

From the shallow bottom surface of the Kitakurose and the Shinkurose Bank, the sediments and rocks were sampled by using the "OKEAN" (G-4, G-5, G-6, G-6', G-7) and a dredge system (D-2', D-3, D-4) for the purpose of making clear the character of the sediments and taking limestone.

3-1. Deep Sea Photographs
3-1-1. The Deep Sea Camera System
During this cruise, photographs on the seafloor were taken successfully at three sites using the deep sea cameras. The block diagram of the system is shown in Fig. 11a. The cameras used in the cruise were Benthos type 372, which enables the taking of 750 shots on 100 feet of 35 mm film. The strobo was a Benthos type 382 electron flash, which has a Ni-Cd rechargeable battery and could take 1,000 continuous shots at 100 Watts. This strobo included a timer, in which the flash starting time was set in advance on board and which also sent a signal to the camera through the cable. The film was wound when the signal was relieved. This process was repeated every six seconds after the observation started
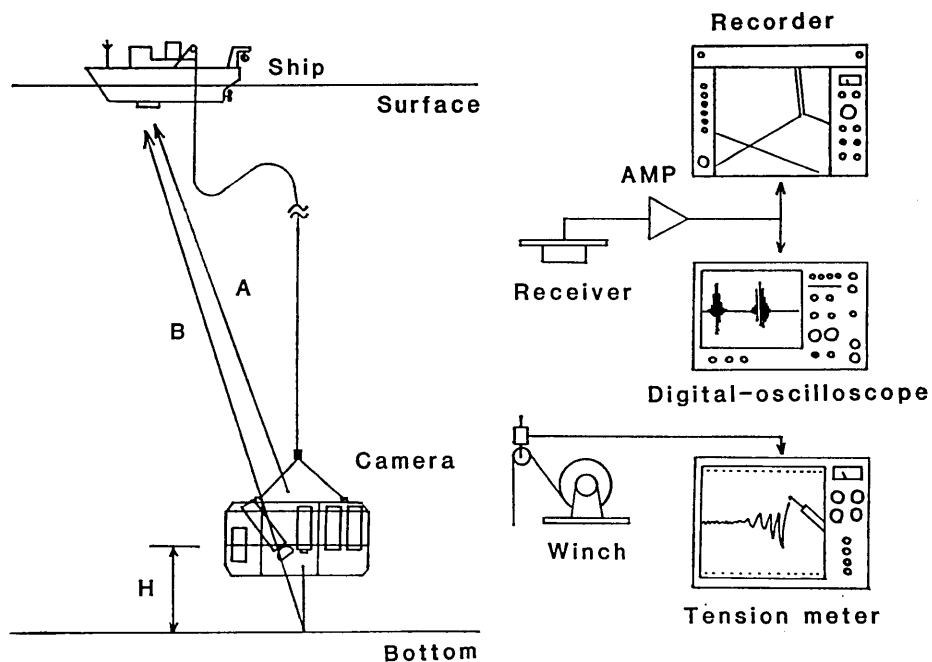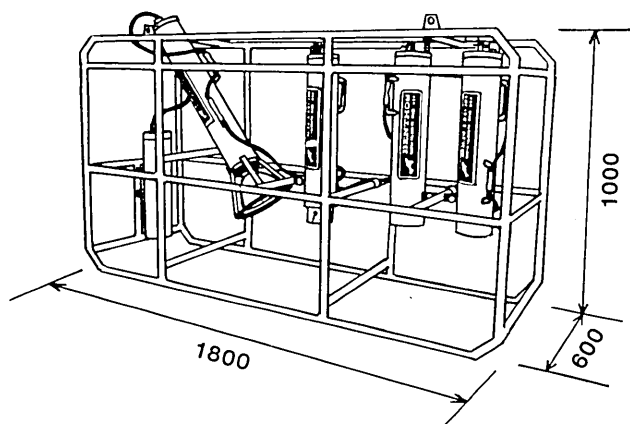
Fig. 11a.

Fig. 11b.

Fig. 11. (a) The block diagram of the deep sea camera system. (b) Sketch of the deep sea camera system employed during the cruise.

on the ocean bottom. Each shot had the date and time in its left corner, by which we could roughly know the shot point from the ship's position.

The cameras were a fixed focus type and the flash not reach more than three meters. Hence, the distance between the cameras and the sea

bottom had to be kept within 1.5-2 m. To know this distance, a pinger was attached to the instrument. It periodically pinged with a 12 kHz pulse, and from the time differnece between the direct signal and the reflected signal from the sea bottom, we could tell the distance between the instrument and the sea bottom. During this cruise a Benthos type 2216 sonar pinger was used, and for detecting the time difference of the acoustic pulses a digital storage oscilloscope was used.

Additionally, an inner water compass made by the Kaiyo Denshi Co. Ltd. was used, but due to the trouble on the stage of the initial adjustment it did not work at all and the photographs did not include direction. This compass receives the synchronized signal from the strobo flash and it in turn sens the information on the time, direction and tilt to the RAM, which is necessary for the analysis of the photographs.

All the instruments were vertically attached to the steel grid which could be lowered over the ship's side (Fig. 11b). The strobo was obliquely equipped in order to reduce the reflected light due to the suspended materials in the water.

The echo from the pinger was received with the PDR receiver of the ship. The height of the cameras was controlled by the winch.

3-1-2. The film

The film, "Sakura 400", was used instead of "Kodak 5294". The sea bottom photographs were taken under the daylight-like strobo, and the Kodak 5294 type (for tungsten) needs some corrections when printed. However, the "Sakura 400" type has not need for correction because it was made for daylight use. The length of the film was just 100 ft so that it was easy to install the cartridge. It also had the merit whereby the difference of the number of the shot between the two cameras diminished. During this cruise, "Sakura 400" was used in camera A and "Kodak 5294" in the camera B in order to compare the resolutions. The result was that no significant differences of the resolution were found except that the "Sakura 400" was slightly darker colored.

3-1-3. The shot sites

One observation was made in the Hachijo Basin and two in the Mikura Basin. In the Hachijo Basin, the cameras were towed toward the western slope of the Kenkenyama Seamount located west of Hachijojima. Because the ship drifted in the tidal current, the instrument could not reach the top of the mountain during its time of operation. The two sites in the Mikura Basin were the thermal anomalies were found by the

CTD towing done before the camera. We tried to go across that very point.

3-1-4. The results

C-1 (The Hachijo Basin; the western slope of the Kenkenyama)

The surveyed area was completely covered with sediment and the fault plane could not be detected. As recognized from the ripple mark in Fig. 12-1. (a), a strong bottom current existed locally. Various kinds of bottom dwelling organisms that eat plankton carried by the current are seen in Fig. 12-1. (b). In some shots, hard rocks cropped out on the slope of the Kenkenyama seamount. Hydrothermally precipitated sediments wereseen in some shots taken by the deep sea camera (Fig. 12-1. c) and gravel consisting of volcanic rocks were also seen (Fig. 12-1. d).

C-2 (The Mikura Basin)

This was one of the sites where anomalies of seawater temperature were found by CTD measurements. Almost all the places were covered with sediment, and on the surface some large and small stripes due to the activities of the benthos were seen (Fig. 12-2. a, b). Small sandy mounds were seen in the photographs which were thought to be made by such bottom dwelling organisms as star fish.

However, various shaped and sized volcanic rocks were cropping out near the water temperature anomaly point found by the CTD (Fig. 12-2. c, d, e). This zones was about 15-20 m long along the track of the deep sea cameras and after crossing the rocky bottom was again covered with thick mud. The various kinds of benthic organisms were actively living on the bottom surface. (Fig. 12-2. f, g, h, i).

C-3 (The Mikura Basin)

This was the other site where anomalous bottom water temperature was found by CTD. Like C-2, this site was completely covered with mud. Near the thermal anomaly point, rocky outcrops were observed (Fig. 12-3. a to l).

The number of benthos was the largest among the three sites, and all kinds of benthos were also shown in the photographs (Fig. 12-3. a to e). An especially large number of sea cucumbers were observed, and sea urchins formed groups (Fig. 12-3. a, c). As observed at site C-2, several shots showing rocky outcrops were seen at site C-3 (Fig. 12-3. f, k, l) which were composed mostly of volcanic rocks that recently erupted on the sea floor, recently.
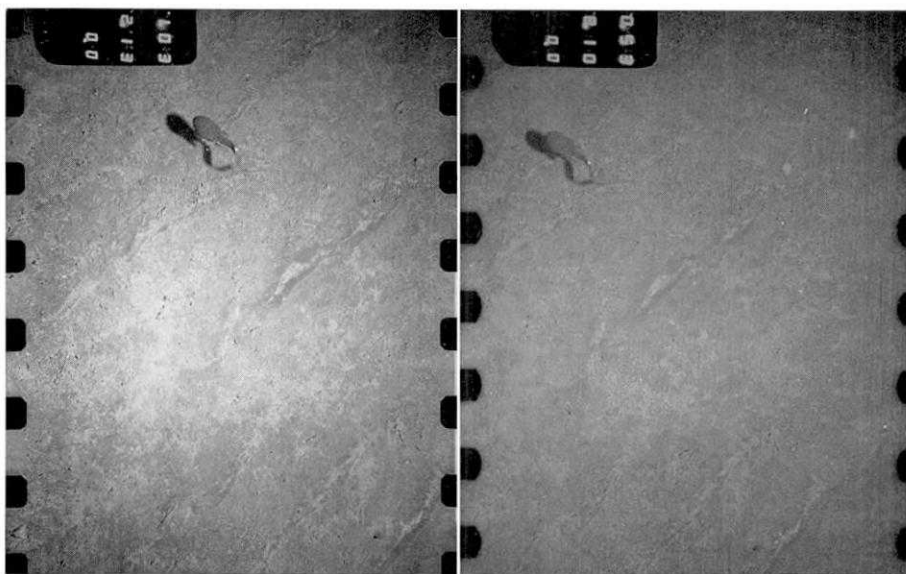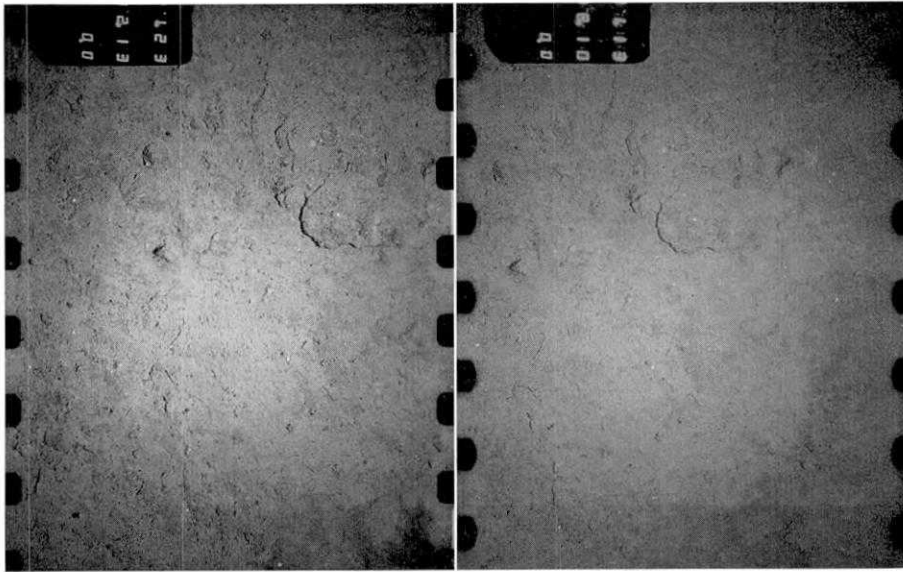
Fig. 12-1a.

Fig. 12-1b.

Fig. 12–1c.
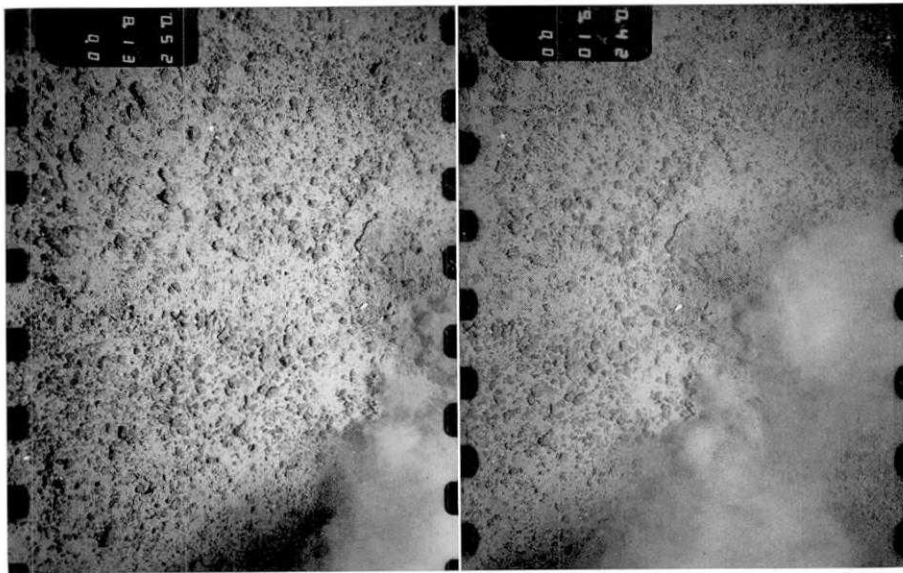
Fig. 12–1d.

Fig. 12-1. Submarine photographs taken from the Kenkenyama Seamount west of the Hachijojima. (a) Ripple mark and fish swimming the ripple. (b) Various kind of bottom dwelling organisms. (c) Thin crust of mudstone covering the foot of the seamount. Note the brown aggregates of the clayey materials being possibly hydrothermal nontronite. (d) Gravel composed mostly of volcanic rocks covering the foot of the seamount. Note white dust of fine materials which may consist of foraminifers.

Fig. 12-2a.

Fig. 12-2b.
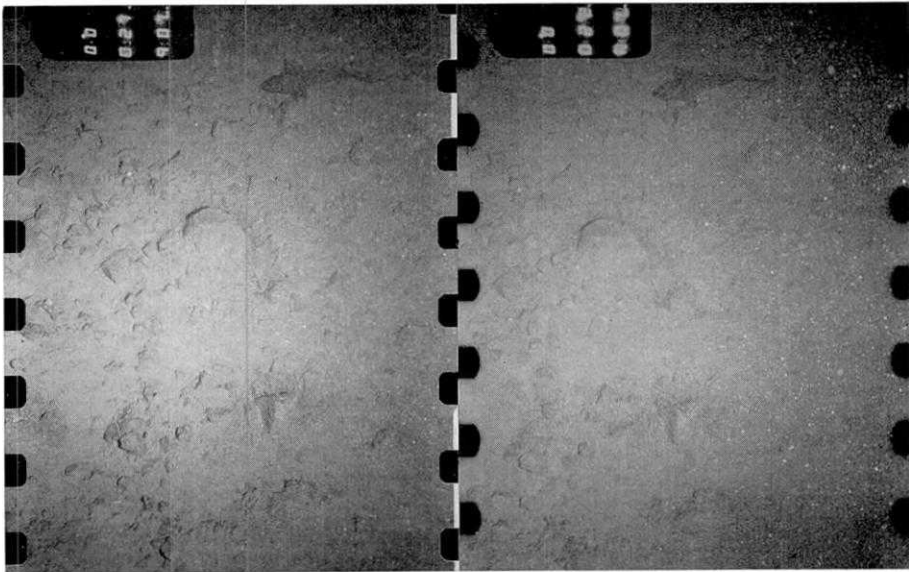
Fig. 12-2c.

Fig. 12-2d.
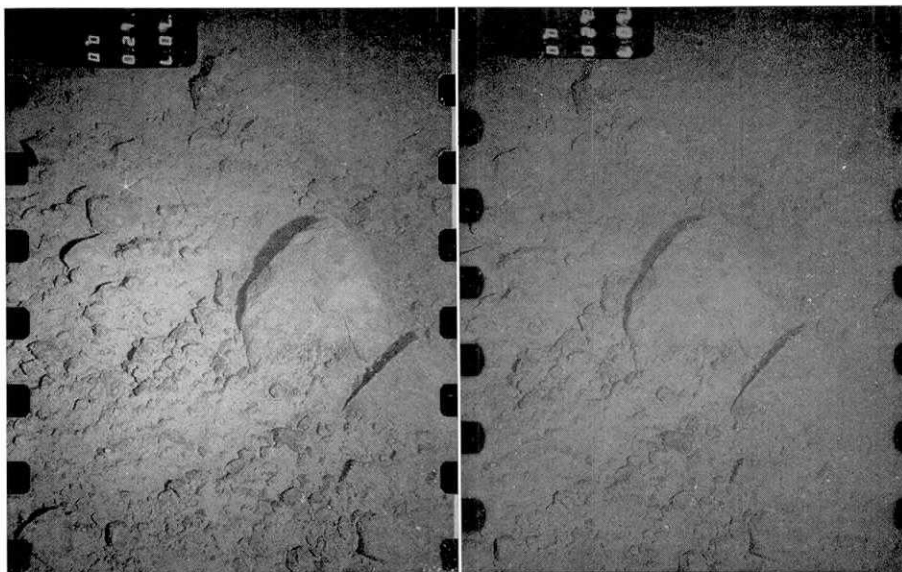
Fig. 12-2e.
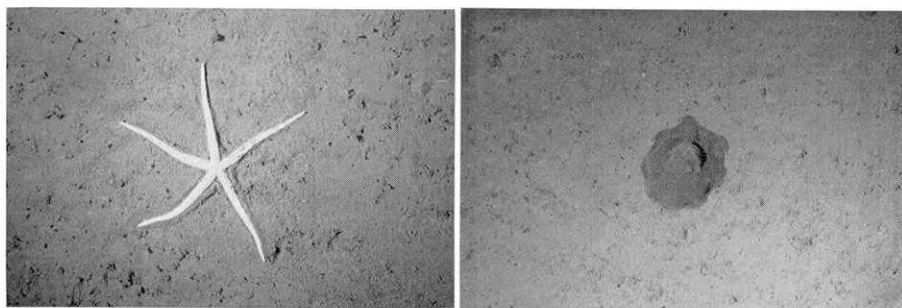
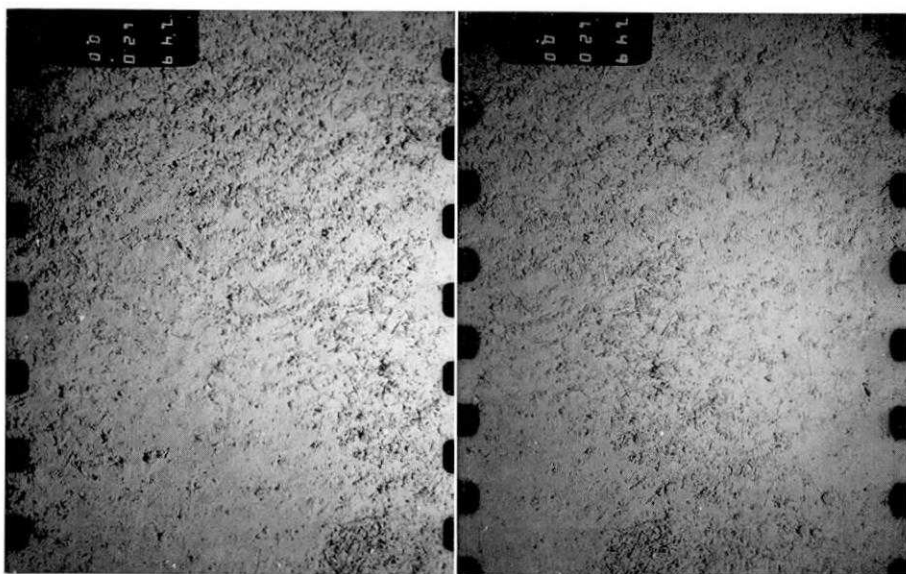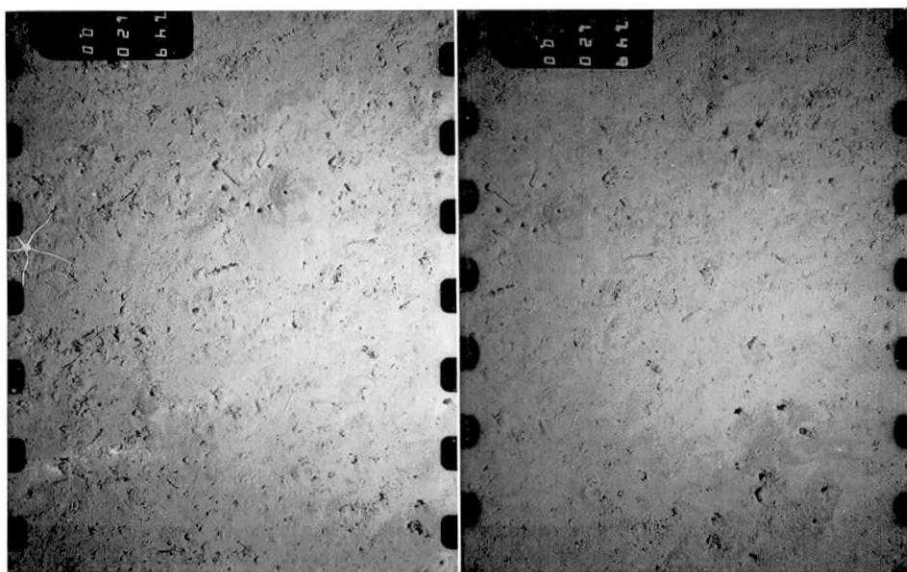Fig. 12-2f.   Fig. 12-2g.

Fig. 12-2. Submarine photographs taken from the bottom of the Mikura Basin. Track
line of the deep sea camera is shown in Fig. 6. (a) Pebbly surface covering the
bottom of the Basin. (b) Small sandy mound made by the bottom dwelling
organisms, star fish, are scattered all over the bottom. (c) Rocky outcrop of the
western foot of the small knoll-like topographic high. (d) Angular blocks of vol-
canic rocks forming the small knoll-like topographic high. (e) Angular cobbles of
volcanic rock covering the western slope of the small knoll. (f) Large star fish
dwelling on the bottom. (g) A kind of octopus living on the bottom. (h) Un-
known white organism swimming in the sea water. (i) Shiny red shrimp and star
fish.

3-2. Dredge

Rock samples were taken by using cylindrical chain bag type dredgers.
Bottom surface finer sediments were also obtained by two or four small

Fig. 12-2h.   Fig. 12-2i.

cylindrical dredgers connected to the main dredger.

D-1 (Western slope of Kenken Seamount)

The major rock type obtained at the foot of the seamount was basalt. Sediments consisted of basalt granules and pebbles, and a matrix of sand and mud. Coarse fraction of the sediments was mainly composed of such volcanogenic materials as scoria and basaltic fragments and small amounts of such biogenic materials as foraminifera and sponge spicule were also found. (Fig. 13a, b).

D-2' (Kurose Bank)

One piece of limestone with algae and fragments of limestone was obtained from the dredge haul of the flat summit of Kurose Bank (depth: 320 m).

D-3, -4 (Shinkurose Bank)

At sites D-3 and D-4, several living sea urchins were collected.

Fig. 12-3. Submarine photographs taken from the eastern part of the small knoll in Mikura Basin. Track line of the deep two camera in shown in Fig. 6. (a) A group of sea urchin walking on the soft bottom sediments. (b) Jelly fish or seacucumbes swimming in the sea water. (c) White sea cucumbers walking on the bottom. (d) A red sea spider trying to enter nest. (e) While sponge dwelling on the sediment surface. (f) Angular cobbles of volcanic rocks covering the eastern slope of the small knoll. Various kinds of bottom dwelling organism live on the rocks. (g) White sea cucumber and brittle star fish. Note the brittle star fish in nest. (h) Brittle star fish barely dig up the bottom sediments of the basin. (i) A group of nests of unknown organisms. (j) Large sea anemone dwelling on the bottom. A small portion of the surface sediments represent a different color from the surrounding sediments. (k) Round and angular cobbles of volcanic rock cover the surface of the bottom. Various kind of bottom dwelling organisms live on the rock. (l) Angular cobbles of volcanic rock covering the eastern slope of the small knoll.
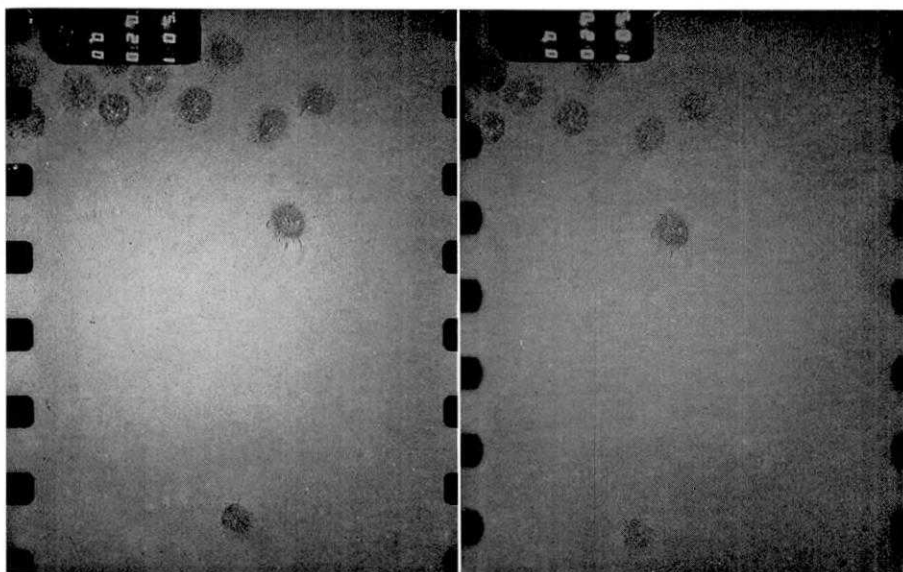
Fig. 12-3a.

Fig. 12-3b.
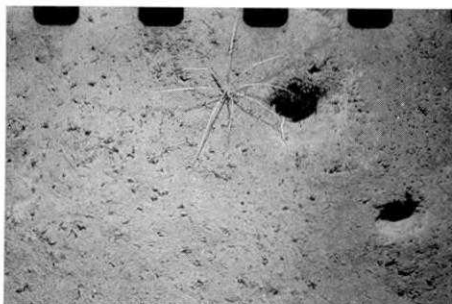

Fig. 12-3c.

Fig. 12-3d.
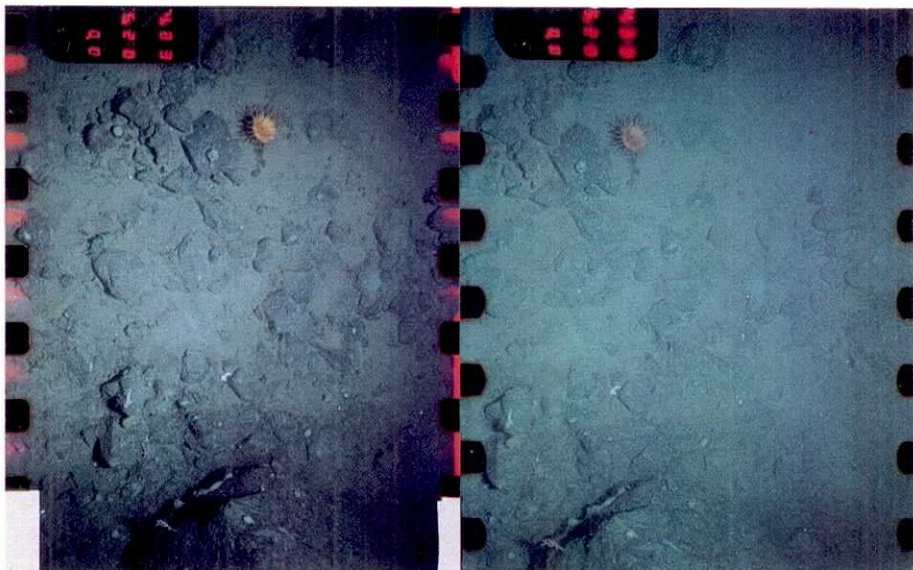

Fig. 12-3e.

Fig. 12-3f.

Fig. 12-3g.

Fig. 12-3h.

Fig. 12-3i.

Fig. 12-3j.

Fig. 12-3k.

Fig. 12-3l.
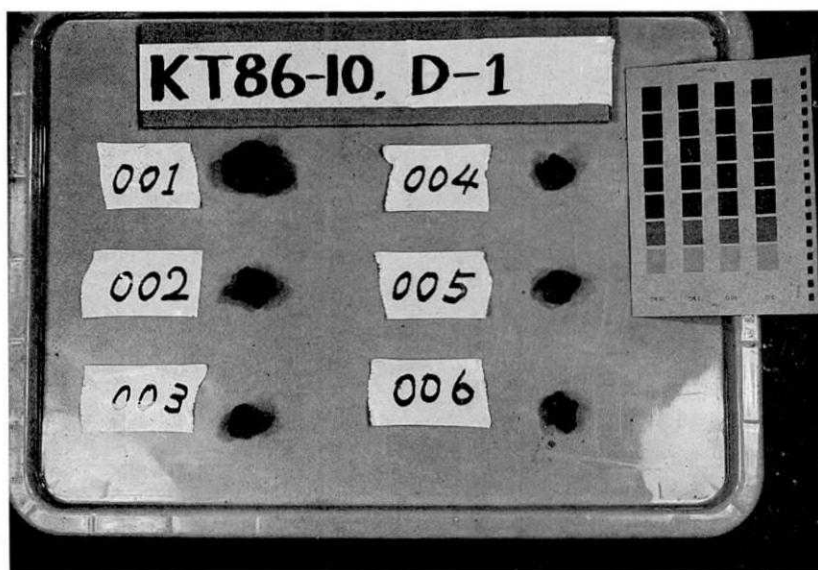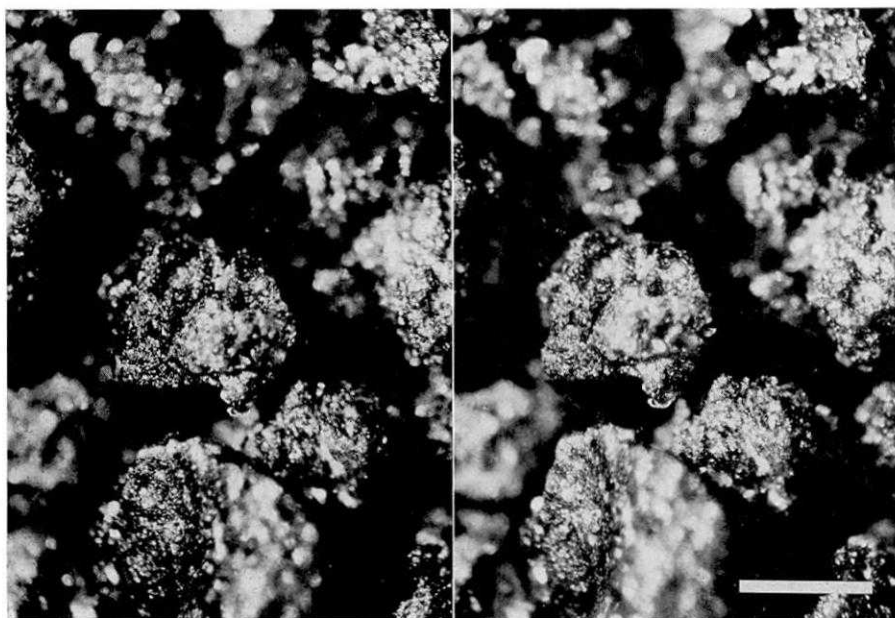
Fig. 13a.

Fig. 13b.

Fig. 13.   Stereographic photomicrograph of the dredge D-1 (scale bar=1 mm).

Sponge and coral fragments were obtained at site D-4.

3-3. Surface sediments

The "OKEAN" type grab sampler was handy in obtaining large amounts of surface samples *in situ* within any trouble. During the cruise this type of grab sampler was used for collecting the undisturbed surface sediments in the surveyed area. The methodology for treating the sampler was the was as described in KH 86-1 (FUJIOKA, *et al.*, 1986).

G-1 (Hachijo Basin)

Surface sediment about 25 cm thick was taken from the central part of the Hachijo Basin at a water depth of 1,294 m. The sediments were dark olive sandy mud in which the layered and spotted sand was encountered in the lower portion. The top of the sediment was composde of calcareous nannofossils, diatoms, foraminifera and silicoflagellates as biogenic components (70%) and volcanic glass shards, feldspars and orthopyroxenes as volcanogenic components. More than 70% of the coarse fractions of the samples consisted of black and red scoria and volcanic glass shards they also contained small amounts of foraminifera and sponge spicules (Fig. 14a). Chondrites and Zoophycos type disturbances were clearly seen on soft X-ray radiographs taken from the sub-core (Fig. 17f).

G-2 (Mikura Basin)

About a 10 cm thick surface sediment was obtained by the grab sampler at the southwestern part of Mikura Basin. The water depth was a grayish olive sandy mud. Volcanogenic materials were feldspars, ortho-pyroxenes, clinopyroxenes, volcanic glasses and scorias, which made up about 60% of the total coarse fraction (Fig. 14b). The biogenic materials were foraminifers and sponge spicules. The muddy part of the sediment contained calcareous nannofossils, diatoms and silicoflagellates.

G-3 (Mikura Canyon)

Samples were recovered from the Mikura Canyon at a 1,693 m depth east of the Shinkurose and Kitakurose Banks. Sediments consisted mostly of biogenic materials whose compositions were foraminifera, sponge spicules and shell fragments (Fig. 14c). Volcanogenic materials consisted of scorias, pumices, volcanic glasses and feldspars. The sediment is scanty of finer matrix but a small amount of mud consisted of calcareous nannofossils, diatom and silicoflagellates.

K. Fujioka *et al.*
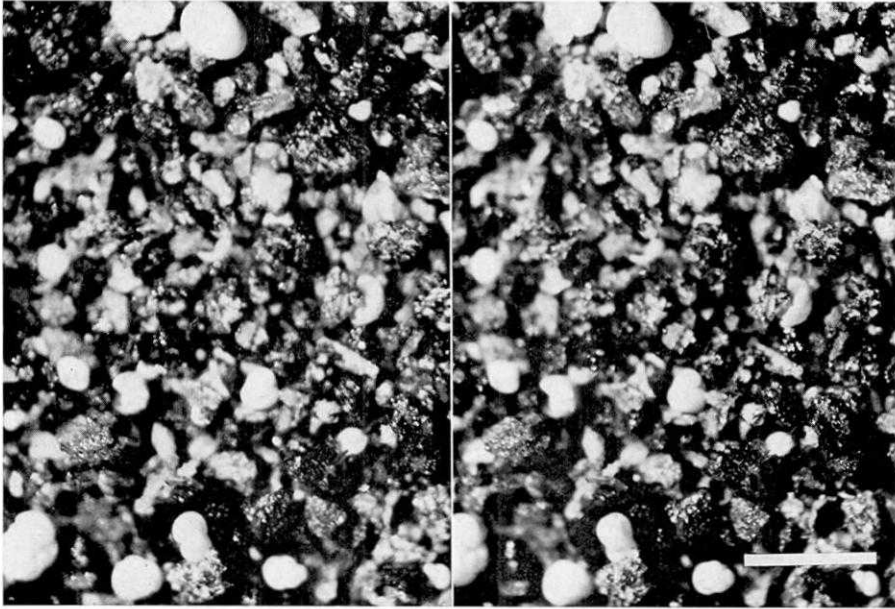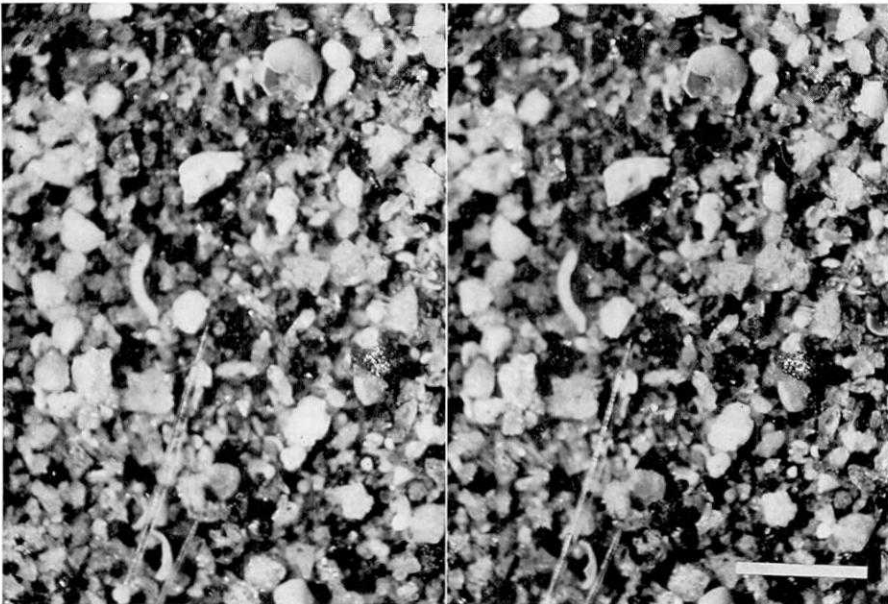
Fig. 14a.

Fig. 14b.

Fig. 14c.

Fig. 14d.

K. Fujioka *et al.*

Fig. 14e.

Fig. 14f.

Fig. 14g.

Fig. 14. (a) Stereograhic photomicrograph of the coarse fraction of the grab G-1 (scale bar=1 mm). (b) Stereographic photomicrograph of the coarse fraction of the grab G-2 (scale bar=1mm). (c) Stereographic photomicrograph of the coarse fraction of the grab G-3 (scale bar=1 mm). (d) Stereographic photomicrograph of the coarse fraction of the grab G-4 (scale bar=1 mm). (e) Stereographic photomicrograph of the coarse fraction of the grab G-5 (scale bar=1 mm). (f) Stereographic photomicrograph of the coarse fraction of the grab G-6 (scale bar=1 mm). (g) Stereographic photomicrograph of the coarse fraction of the grab G-7 (scale bar=1 mm).

G-4, -5, -6, -6' (Kitakurose Bank)

Sediments on the Kitakurose Bank consisted of such biogenic materials as foraminifers, shell fragments and coral fragments and such volcanogenic materials as scorias and pumice (Fig. 14d, e, f). The surface of the foraminifers were stained pale brown indicating that the forams were affected by the hydrothermal activity that possibly took place in a nearby area and the precipitation of manganese materials on the surface.

G-7 (Shinkurose Bank)

Samples were taken from the flat summit of the Shinkurose Bank at a 184 m water depth. Materials consisted of such biogenic remains as foraminifers and limestone fragments. Small amounts of scoria and volcanic glass shards were also obtained (Fig. 14g).

3-4. Piston core sediments

A new type of piston core system developed by K. FUJIOKA and K. KOGA was used. It has a four or eight meter stainless steel core barrel, a 82 mm inner diameter, and weighed about 500 kg. An inner tube cut lengthwise beforehand was used during the cruise. The sites for piston coring are given in Figs. 5 and 6 and in Table 1.

Thermal conductivity of the sediments was measured on the columner sediments of the piston core 12 hours after equilibration of the sediment temperature with the room temperature. Core samples were into two halves: archive and working. The archive half was used taking core photographs (Fig. 15a) and visual core descriptions (Fig. 15b) before storage. The working half was first treated for soft X-ray radiograph. Thin sediment slices were cut out and stored in plastic cases ($200 \times 80 \times 8$ mm). Soft X-ray radiographs were taken under the condition of 45 kV, 12 mA, and 25 sec. for all the core samples. Smear slides were prepared for the petrographic examination with all the dominant lithologies. For the study of the calcareous nannofossils and other microfossils a one centimeter thick portion of these cores was taken at stratigraphic intervals of 10 cm through the cores. The experimental treatise of the columner sediments taken by piston coring was the same as described by FUJIOKA *et al.* (1986).

PC-1′ (Hachijo Basin)

A 111 cm long core of grayish olive and gray fine sand and mud was recovered. The sand parts mainly consisted of volcanic glasses, scoria and feldspars with a small amount of orthopyroxenes and clinopyroxenes as heavy minerals (Fig. 16a). In the muddy parts, many calcareous nanno-fossiles and foraminifers predominated.

Sediment on the top of the pilot core showed sea bottom surface, which was composed of dark olive mud. Biogenic materials consisted of calcareous nannofossils, foraminifers, sponge spicules, diatoms, silicoflagellates and radiolarians. These biogenic materials accounted for more than 70% of the surface sediments. Volcanogenic materials were composed mainly of volcanic glasses and feldspars. Orthopyroxenes and clinopyroxenes were also seen in the bottom surface sediment.

On the soft X-ray radiographs of this core sample, the vertical lamination due to flowing in the inner tube after coring was observed. However, we could see the Zoophycos and Chondrites type bioturbances in the top part of the radiographs (Fig. 17a).
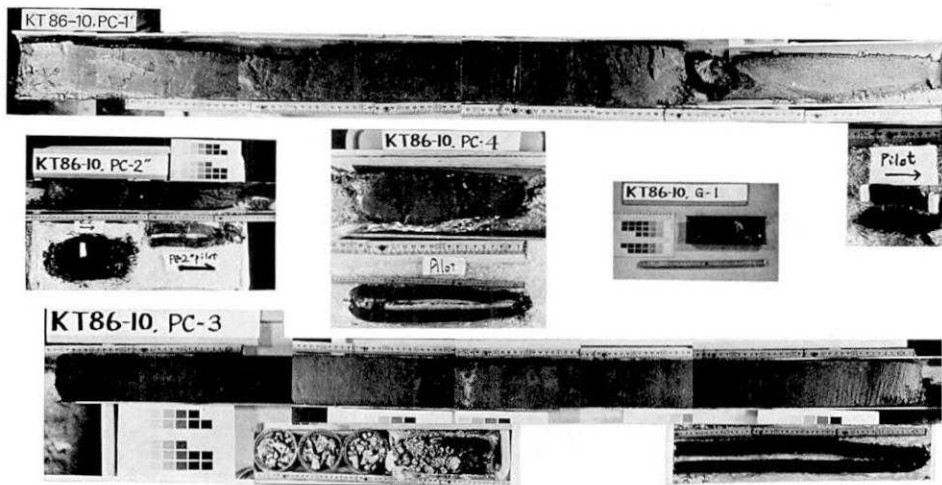
Fig. 15a.
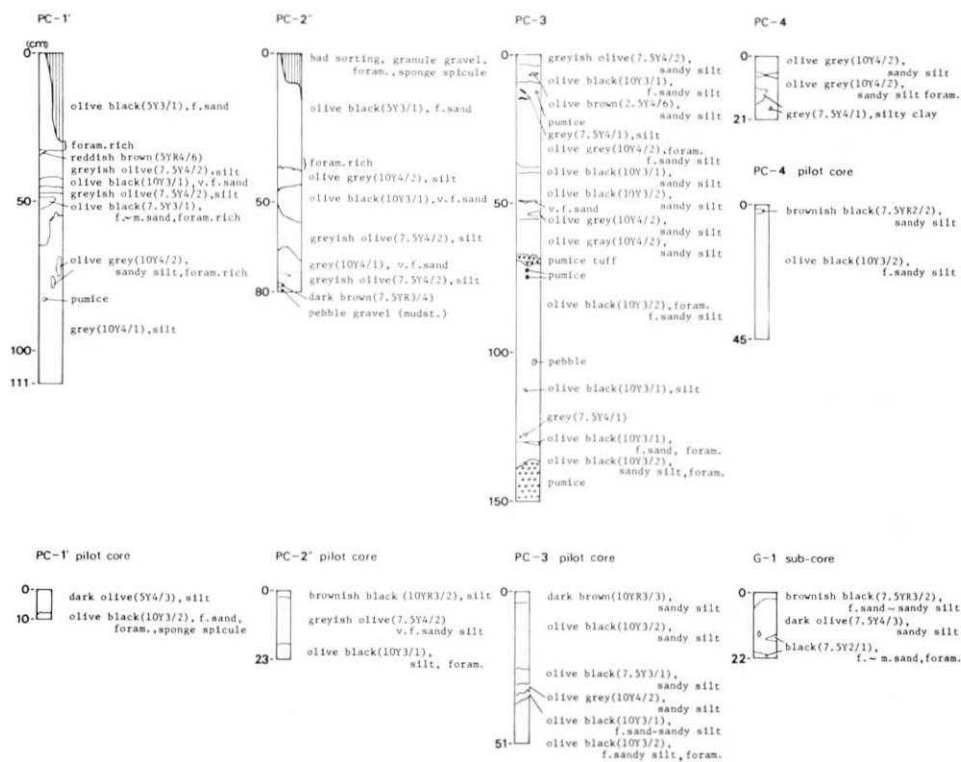
Fig. 15b.

Fig. 15.   (a) Photograph of the piston core.   (b) Piston core description.

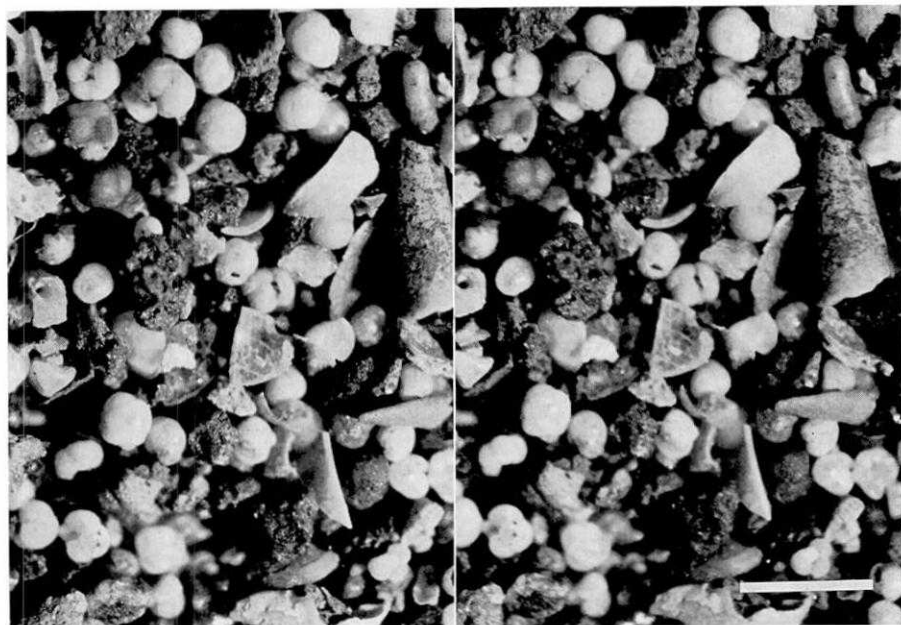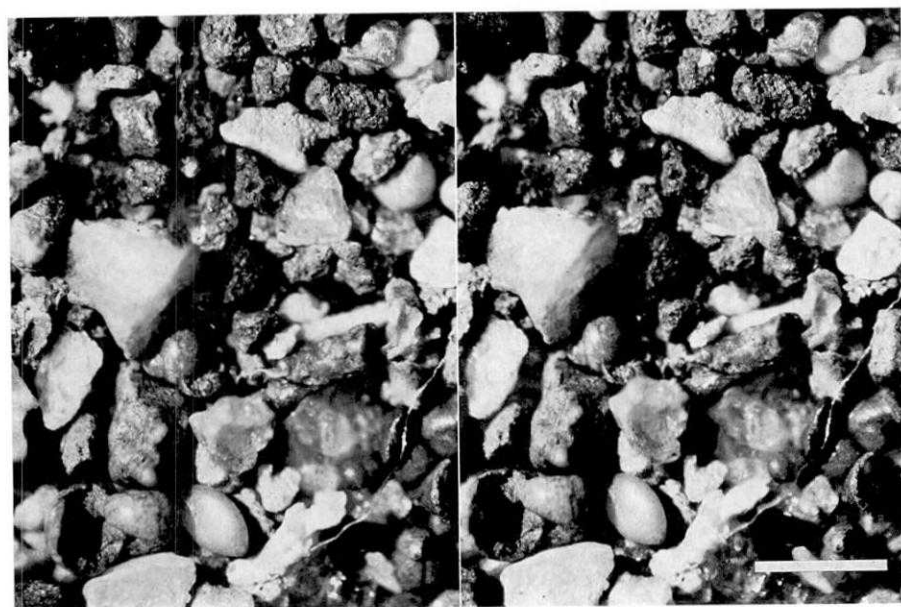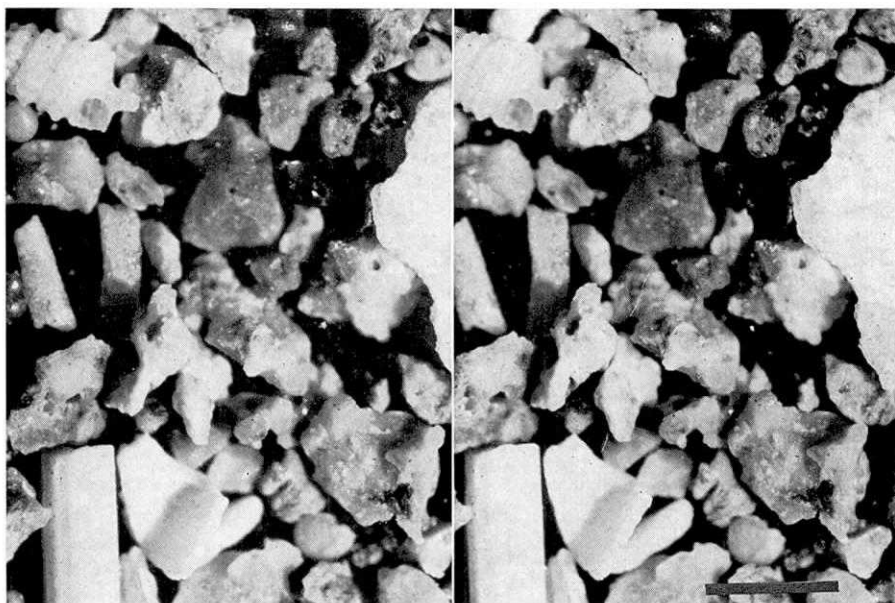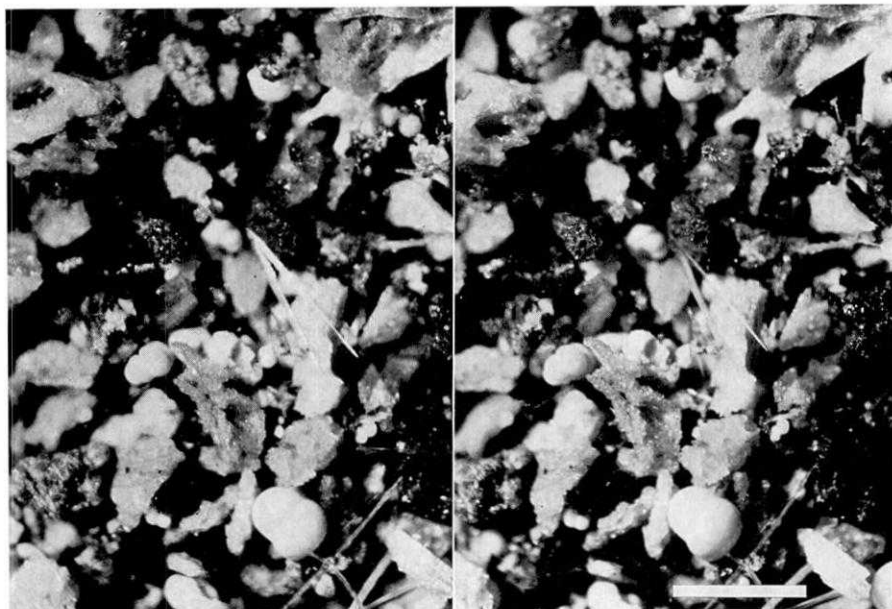Fig. 16a.
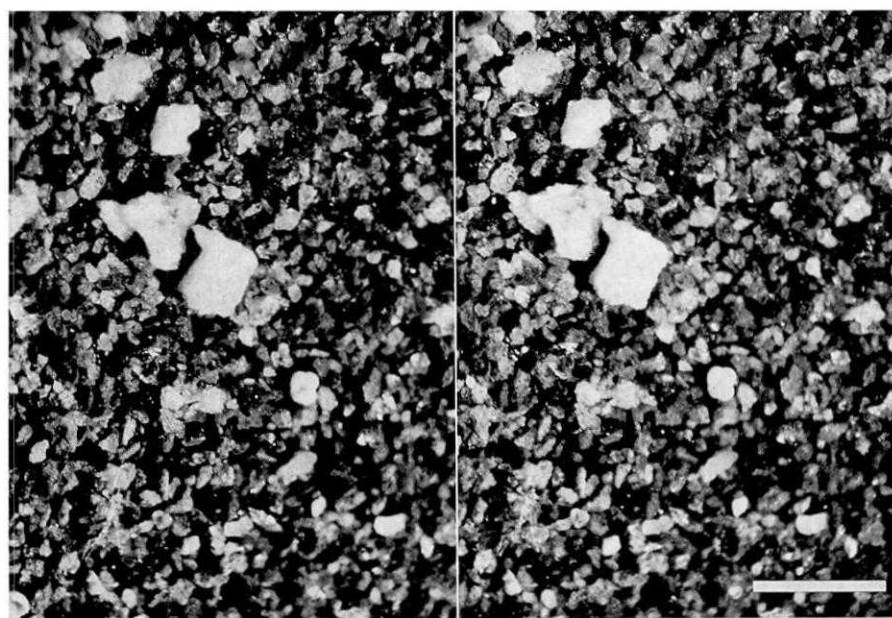
Fig. 16b.
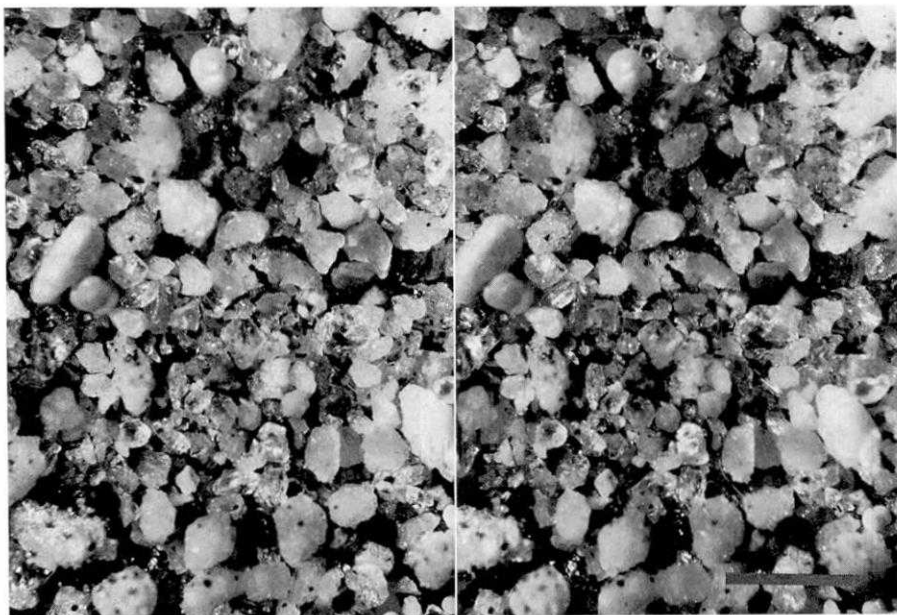
Fig. 16c.

Fig. 16. (a) Stereographic photomicrograph of coarse fraction of the piston core P-2″ (scale bar=1 mm). (b) Stereographic photomicrograph of coarse fraction of the piston core P-3 (scale bar=1 mm). (c) Stereographic photomicrograph of coarse fraction of the piston core P-1′ (scale bar=1 mm).

PC-2″ (Mikura Basin)

This core was obtained from the western Mikura Basin floor west off Inanbajima. Dark grayish olive sand, silt and granules with a length of 80 cm were recovered at the station. The sediment was flown in the inner tube after coring, such as core P-1′. Such volcanogenic material as feldspars, orthopyroxenes, clinopyroxenes and volcanic glasses made up more than 70% of the total coarse fractions (Fig. 16b). Small amounts of foraminifera were also contained in coarse fractions as biogenic material. The muddy part of the sediments consisted mainly of calcareous nannofossils and small amounts of diatom, silicoflagellates and sponge spicules.

The sediment of the top of the pilot core was composed of blackish brown silt and clay. Biogenic materials made up almost 70% of all the sediments and consisted of calcareous nannofossils, foraminifers, sponge spicules, diatoms, radiolarians and silicoflagellates. Volcaniclastic materials consisted of volcanic glasses, feldspars, orthopyroxenes and clinopyroxenes.

Thin lamination as a sedimentary structure and Chondrites type burrows as a bioturbation structure were partly observed on the soft X-ray radiographs (Fig. 17b).

17(a)   PC-1′, 30-110 cm
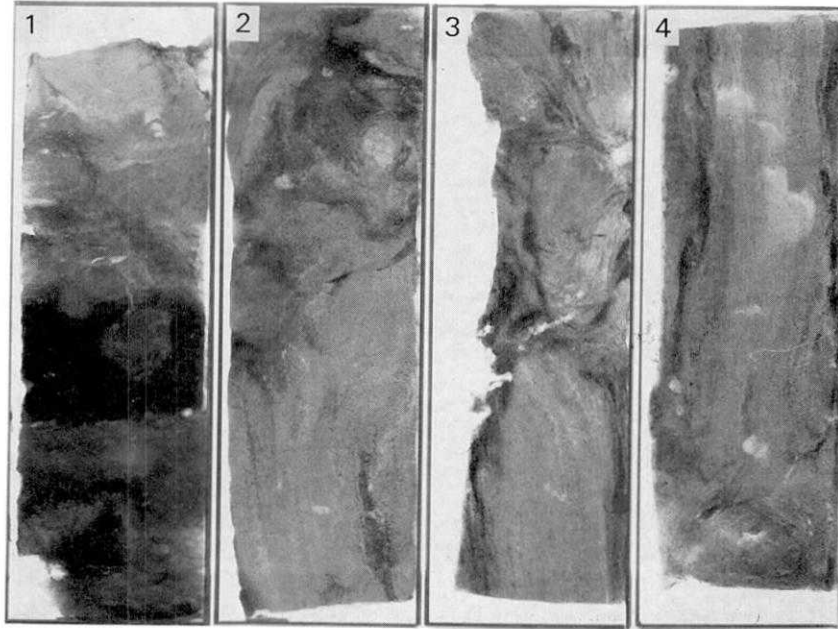
17(b)   PC-2″, 10-61.5 cm
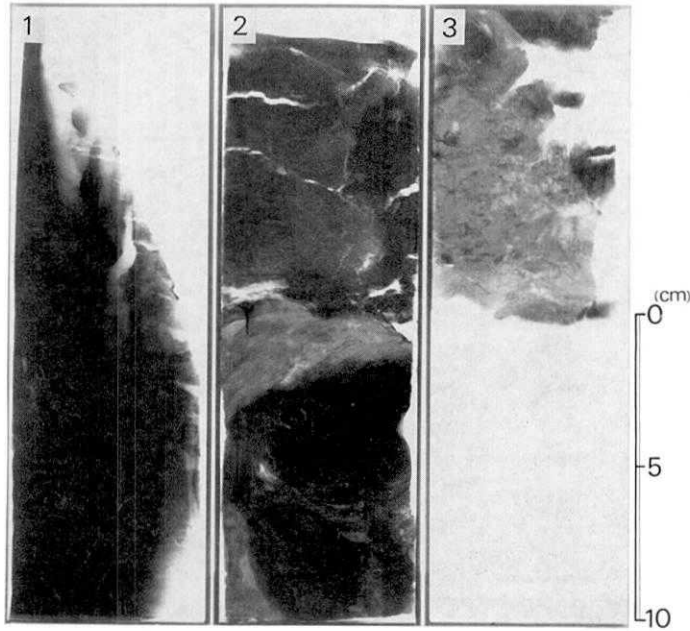
17(c) PC-3.0-138cm
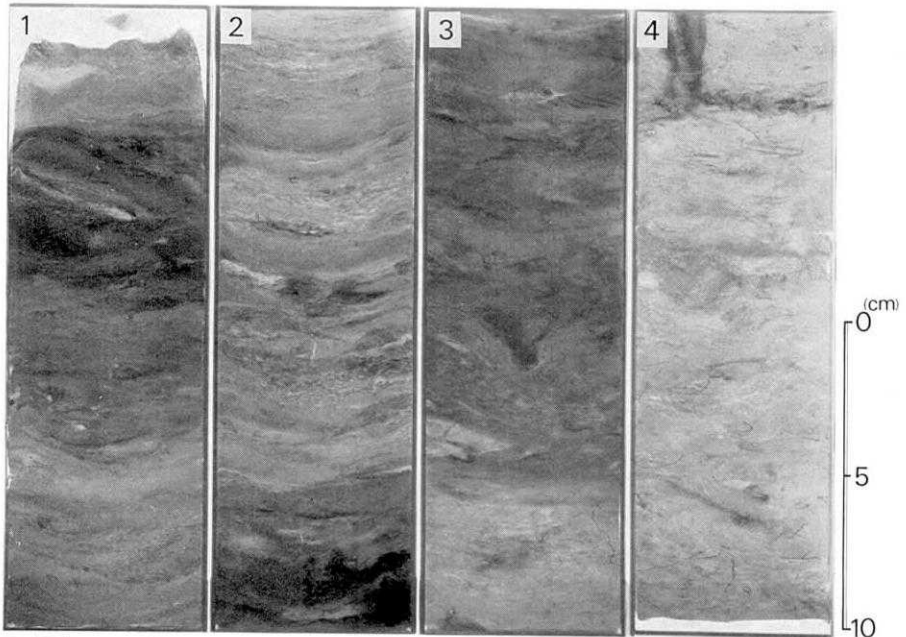
PC-3(cont.)
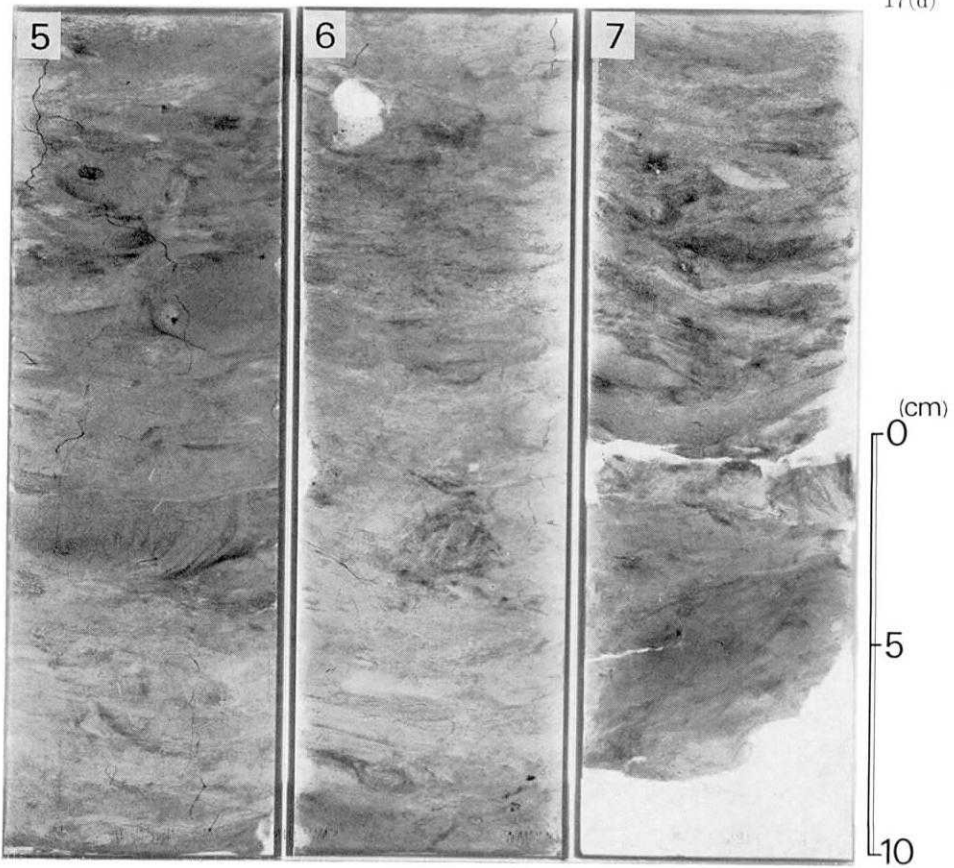
17(d)

17(e)   PC-3,Pilot core, 0-51cm
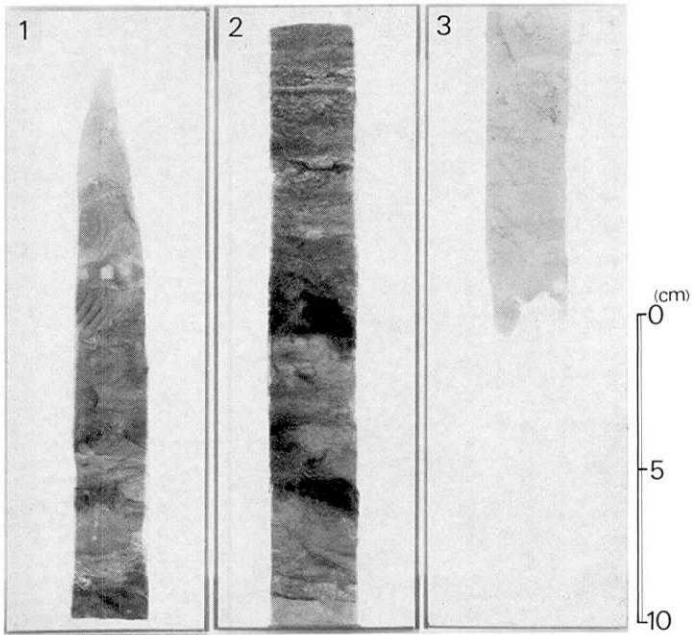
17(f)   PC-4   PC-4,Pilot core, 0-45cm   G-1,Sub core
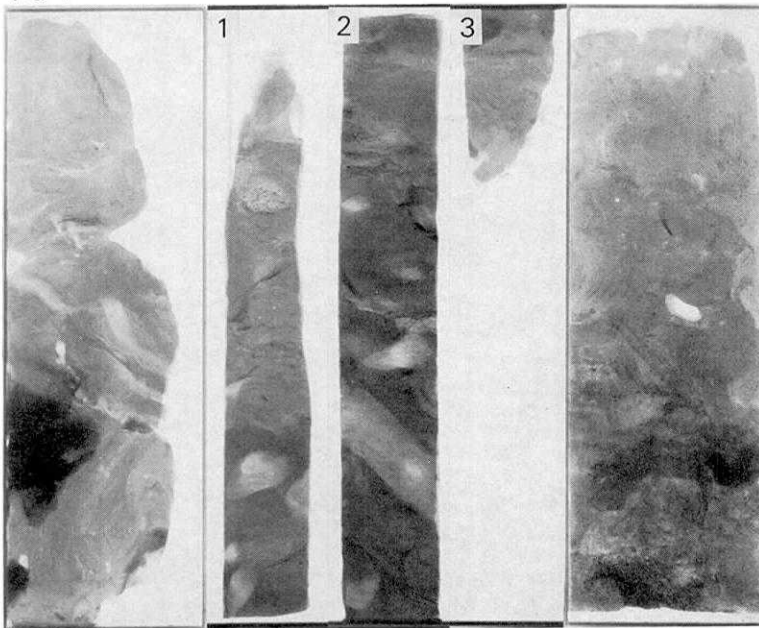
Fig. 17.   Photograph of the soft X-ray of the piston core.

PC-3 (Izu-Ogasawara forearc slope)

Dark olive sandy silt with a length of 150 cm was recovered on the slope of the Izu-Ogasawara forearc east of the Kurose Bank. The sediments were intercalated by thin pumiceous ash layers and pumice fragments. The sandy parts were almost completely composed of volcaniclastic materials (Fig. 16c), consisting of volcanic glasses, feldspars, orthopyroxenes, clinopyroxenes and hornblendes. The muddy parts consisted mostly of diatoms and sponge spicules, and small amounts of calcareous nannofossils, radiolarians and silicoflagellates. In the bottom part of the core (135 cm–150 cm) fresh massive pumice was obtained (Fig. 15a).

The bottom surface sediment was taken by pilot corer, which was composed of dark brown sandy silt, Biogenic materials made up almost 65% and consisted mainly of calcareous nannofossils, sponge spicules, diatoms, and small amounts of radiolarians and silicoflagellates. Volcanic glasses, feldspars, orthopyroxenes and clinopyroxenes were also predominate in the surface sediment.

Many bioturbation structures were observed throughout the core as well as the pilot core based on soft X-ray radiograph (Fig. 17c, d, e). Disturbances of the Zoophycos type, the Planolites type and the Chondrites type were recognized. Cross and parallel laminations were also developed.

PC-4 (Mikura Basin)

Twenty one centimeters of grayish olive sand and silt was taken at the station. The sandy part of the sediments consisted of volcanic glass, feldspar, orthopyroxenes, clinopyroxenes and some foraminifers. Almost all of the muddy part consisted of calcareous nannofossils, sponge spicules and diatoms.

The top sediments of the pilot core was composed of blackish brown sandy silt. Biogenic material made up about 75% of the total sediments, which were made up of calcareous nannofossils, sponge spicules, diatoms, foraminifers and silicoflagellates. Small amounts of volcanogenic materials consisting of glass shards, feldspars, orthopyroxenes and clinopyroxenes were also observed under the microscope.

The soft X-ray radiographs shower sedimentary structures partly of Chondrites type burrows (Fig. 17f). Sedimentary structures were disturbed were disturbed by flow in the inner tube after coring. Disturbance by Arenicollites type burrows was clearly seen on the soft X-ray radiograph of the pilot core (Fig. 17f).

Table 2.   List of nannofossils in the surface sediment of the surveyed area during the KT 86-10 cruise.

Sample (interval in cm)	G-1 (0-1)	G-2 (0-1)	G-3 (0-1)	PC-1' (109-110)	PC-2" (79-80)	PC-3 (137-138)	PC-4 (0-1)	PC-4 pilot (44-45)	D-1
Abundance	A	A	A	A	A	A	A	A	A
Preservation	G	G	G	G	G	G	G	G	G
Calcidiscus leptoporus (Murray and Blackman) Loeblich and Tappan	R	R	R	R	R	R	R	R	R
Ceratolithus cristatus Kamptner		+	+			+		+	+
Coccolithus pelagicus (Wallich) Schiller		+	+			S		+	+
Crenalithus spp.	+	+	+	+	+	S	S	S	+
Discoaster variabilis Martini and Bramlette								(+)	
Emiliania huxleyi (Lohmann) Hay and Mohler	A	A	A	A	A	A	A	A	A
Florisphaera profunda Okada and Honjo	C	C	C	A	C	F	A	A	A
F. Profunda elongata Okada and McIntyre	S	S	S	F	S	S	S	R	S
Gephyrocapsa caribbeanica Boudreaux and Hay			+			+			
G. oceanica Kamptner	C	A	C	F	F	C	F	F	F
Gephyrocapsa spp. (small)						+			
Helicosphaera carteri (Wallich) Kamptner	S	S	S	S	S	S	S	S	S
H. hyalina Gaarder	+	+	+	+	+		+	S	
H. wallichii (Lohmann) Boudreaux and Hay	+	+	+	+	+		+	+	+
Neosphaera coccolithomorpha Lecal-Schlauder	+	+	+		+		+		+
Pontosphaera discopora Schiller									+
P. japonica (Takayama) Nishida		+						+	
P. syracusana Lohmann	+					+			+
Pseudoemiliania lacunosa (Kamptner) Gartner	(+)				(+)	(+)			
Rhabdosphaera clavigera Murray and Blackman	+		+	+	+	S	+	+	+
Scapholithus fossilis Deflandre	+		S	+	S	S		+	+
Syracosphaera spp.	+	+	S	S	S	R	+	S	S
Thoracosphaera spp.			+		+				+
Umbellosphaera irregularis Paasche	+	+	+	+	+	+	+		+
U. tenuis Paasche	+		+	+	+	+	+	+	+
Umbilicosphaera hulburtiana Gaarder	+	+	+			+	+		+
U. sibogae (Weber-van Bosse) Gaarder	R	R	R	R	R	R	R	R	S

+<1%, 1%<S<3%, 3%<R<5%, 5%<F<20%, 20%<C<30%, 30%<A,
( ): Reworked specimens

3-5. Age of the sediments

Surface sediments (G-1, G-2, G-3) were obtained from three sites with the "OKEAN", four piston core samples (PC-1′, PC-2″, PC-3, PC-4) were recovered by the piston corer, and slope sediment (D-1) obtained by the small dredger during the KT 86-10 cruise were carefully examined for the biostratigraphy of calcareous nannofossils. For the nannofossil biostratigraphic study, the smear slides were examined under a binocular polarizing microscope at a magnification of 1,500x. Three hundred specimens on slides were identified and counted at random and listed in order to determine the relative frequency of occurrence of the species. The relative frequency was designated by using one of the following codes: A=abundant (more than 30% of the species in total assemblage), C=common (30-20%), F=few (20-5%), R=rare (5-3%), S=slight (3-1%), and +=present (less than one percent and found but not counted). (Table 2)

The tops and bottoms of the four cores were assigned to the Gartner's (1977) *Emiliania huxleyi* Acme Zone (0.07 Ma-Recent). *Emiliania huxleyi* were dominant and made up more than 30% of the total assemblage. Small amounts of *Pseudoemiliania lacunosa* occurred in the interval 0-1 cm of G-1, 109-110 cm of PC-1′, and 79-80 cm of PC-2″. This species was reworked from the Early Pleistocene sediments.

The assemblage of calcareous nannofossiles was characterized by large quantities of *E. huxleyi*, *Gephyrocasa oceanica*, and *Florisphaera profunda*. These three species made upmore than 90% of total assemblage in the sample. *Coccolithus pelagicus* is one of cold water species that occurred in the bottom surface sediments such as G-1 (0-1 cm), G-3 (0-1 cm), and PC-4 (0-1 cm). *Calcidisus leptoporus*, *Helicosphaera carteri*, and *Vmbilicosphaera Sibogae* all occur in all the samples. These species made up 1-5% of the total assemblage. *Syracosphaera* spp. was also found in all the samples and made up 0.6-5% of the total assemblage.

4. Heat flow measurements

4-1. Introduction

So far heat flow measurements in the Izu-Ogasawara backarc area have mainly been made south of Torishima (Ogasawara Trough, Shichito-Iwojima Ridge and Nishinoshima Trough) and in the Shikoku Basin (Fig. 18). Very few measurements were made in the northern part from Sumisujima up to Hachijojima and Miyakejima. Very little data existed around the Mikura Basin area where the measurements were attempted in this study (e. g. WATANABE, 1970).

18(a)

18(b)

Fig. 18. (a) Bathymetric map in the Izu-Ogasawara area. The surveyed area is enclosed in the square. (b) Previous heat flow data in the same area as Fig. 18(a).

The heat flow profile across the Izu-Ogasawara trench-arc system basically shows the same pattern as other normal subduction zones such as the Japan Trench; low heat flow between the trench and the volcanic front, and on the western side of the Shichito-Iwojima Ridge (volcanic arc) heat flow becomes high and variable (VAQUIER, *et al.*, 1966; WATANABE *et al.*, 1977). ANDERSON (1980) suggested that the heat flow in the forearc region was not uniformly low, but its lowest was between the trench and the volcanic front and it got higher as it moved landward from there. He related this feature to the generation of boninites.

MATSUBARA (1981) recently measured the heat flow over the backarc area around 26°N to 28°N, and, in addition to the features noted above, indicated the possibility of hydrothermal circulation in the backarc area just west of the volcanic front, based on the variability in the heat flow there. This backarc area was termed the backarc depression by TAMAKI *et al.* (1981), which was divided into four segments; the Nishinoshima Depression, the Torishima Depression, the Sumisu Depression and the Hachijo Depression. YAMAZAKI (1985, 1986) reported the results of heat flow measurements at all these depressions except for the Hachijo Depression. He suggested that at these depressions hydrothermal circulation occurred based on the observation that in each area the nonlinear temperature gradient existed and that high and low heat flow was found close to each other.

During the cruise of KT 86-10, measurements were attempted around the Mikura Basin which is located in the northernmost part of these backarc depressions. The main objective was to examine if such hydrothermal activity as mentioned above was occurring in this area. However, as pointed out by WATANABE *et al.* (1970), the water depth around here was shallow (about 1,800 m) and the bottom was hard and coarse, and it was anticipated that there would be great difficulty in heat flow measurements. After all, these difficulties were not perfectly overcome and no heat flow values were determined in the Mikura Basin area. However, the anomalous temperature profile was found in some measurements.

Measurements were also tried in the Hachijo Basin and on the eastern side of Kitakurose located in the forearc region.

4-2. Method of the heat flow measurements

Heat flow value is given as the product of temperature gradient and thermal conductivity. At the bottom of deep sea measured surface heat flow directly reflects the thermal state at depth because usually no disturbing factors to affect the surface heat flow (temperature in the sediment

near the surface) exist there.

For the measurements of the temperature gradient we used the Ewing type probe which had been in use in ERI since 1983 (YAMANO, 1985). The electronics were made by the Lamont-Doherty Geological Observatory of Columbia University. It weighed about 450 kg. As seen in Fig. 19, it had six sensors (thermistors) outriggered at regular intervals and had two versions; lance 4.5 m long (for HF-1) and lance 3 m long (for HF-2, 3, 4).

The lances were made of a strong steel rod which was usually used for boring. It allowed multiple penetrations into the sediment. This drastically improved the efficiency of the data collection and enabled closely spaced measurements.

The data was logged in a digital form (12 bit) and recorded serially in a cassette tape every 30 seconds for each sensor, and at the same time these logged data were telemetered to the ship with 12 kHz acoustic pulses. The logged data and telemetered signals also included the information about the instrument tilt, by which, together with temperature information, we could know if the probe penetrated vertically or not, and it was possible to try again soon when the penetration was unsuccessful.

When the probe penetrated, each sensor was frictionally heated. Therefore, we left the probe in the mud after the penetration for ten to fifteen minutes and measured the change in temperature to know the equilibrium temperature in the sediment according to the formulation by BULLARD (1954). This estimated equilibrium temperature includes an error
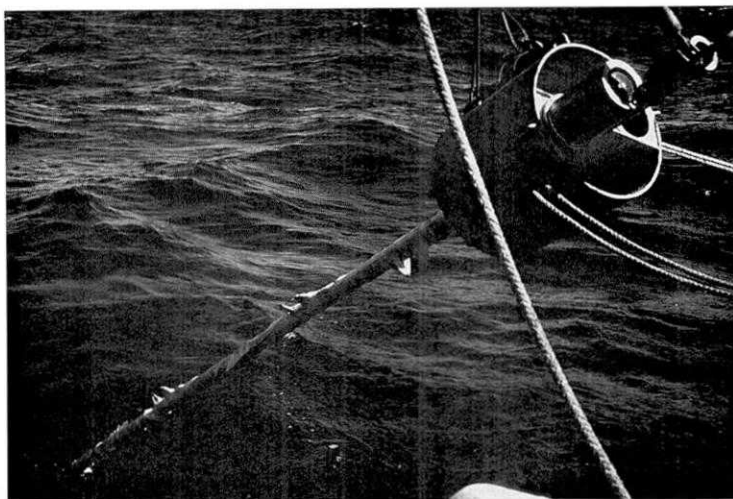
Fig. 19. The Ewing type geothermal probe (4.5 m).

of 0.001 to 0.005 deg. Furthermore, the water had a temperature gradient of about 0.05 deg/30 m around the surveyed area near the sea bottom (temperature was lower near the bottom), which should have caused an error of 0.001–0.002 deg between the temperature differences of each sensor. After all, the relative precision of the temperature was about 0.01 deg. The temperature gradient was calculated by the least square fit of the temperature difference for each sensor versus depth to a straight line.

Thermal conductivity was measured by the needle probe method (VON HERZEN and MAXWELL, 1959) for the core samples taken at P-3 (see Fig. 20) by the piston corer (four meter type which needs the inner tube). The core sample was about one meter long. It was left vertical after taken to equilibrate to the room temperature, and measurements were made twice every 30 cm, taking care of not losing the inner water. This value was corrected for the in-situ pressure and temperature conditions, following RATCLIFFE (1960).
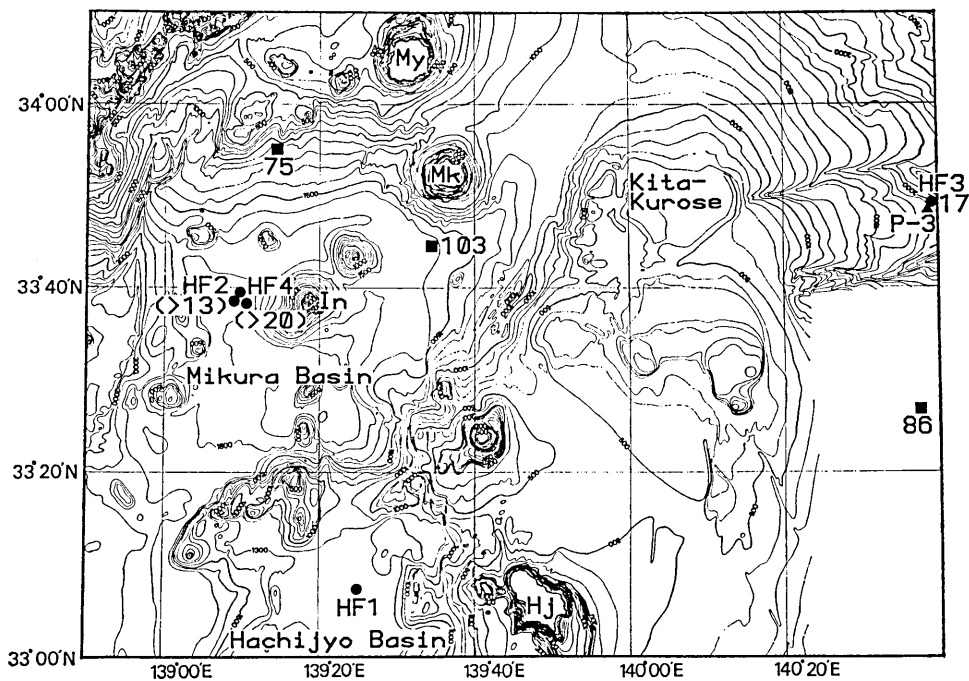
Fig. 20. Heat flow stations and values (HF1–HF4). Unit: mM/m². Solid squares: previous measurements, solid circles: measurements during this cruise, P-3: the piston core station, My: the Miyakejima., Mk: the Mikurajima., In: the Inanbajima., and Hj: the Hachijojima.

K. FUJIOKA *et al.*

4-3. Results and Discussion

We tried to measure the temperature gradient at four stations, as plotted in Fig. 20 together with heat flow values. All the results are listed in Table 3. The obtained temperature versus depth profiles are shown in Fig. 21. Except for HF-3A and HF-3D, the temperature data

Table 3. List of heat flow measurements during the KT86-10 cruise.

| Station	Latitude (N)	Longitude (E)	Depth (m)	PEN (m)	N	G (mK/m)	K (W/m/K)	Q (mW/m²)
KT8610HF1A	(33°07.6′	139°24.5′)	1292	fell				
1B	33°07.6′	139°24.5′	1292	fell				
1C	33°07.5′	139°24.5′	1292	fell				
HF2A	(33°38.3′	139°09.1′)	1875	fell				
2B	33°38.3′	139°09.1′	1875	tilt	(3)	(>20)	0.67*	(>13)
2C	33°38.2′	139°09.3′	1875	tilt	(3)	(>22)	0.67*	(>15)
2D	(33°38.2′	139°09.4′)	1875	tilt	(3)	(>22)	0.67*	(>15)
2E	33°38.1′	139°09.5′	1875	fell				
HF3A	33°48.6′	140°38.6′	1900	2.1	3	20	0.83	17
3B	33°48.6′	140°38.6′	1900	tilt	(3)	(27–34)	0.83	(22–28)
3C	33°48.6′	140°38.6′	1900	tilt	(3)	(18–23)	0.83	(15–19)
3D	33°48.6′	140°38.7′	1900	1.6	3	19	0.83	16
3E	33°48.6′	140°38.7′	1900	tilt	(3)	(22–28)	0.83	(18–23)
HF4A	33°38.4′	139°09.6′	1883	tilt	(2)	(>53)	0.67*	(>36)
4B	33°38.4′	139°09.6′	1883	tilt	(2)	(>34)	0.67*	(>23)
4C	33°38.4′	139°09.6′	1883	tilt	(2)	(>64)	0.67*	(>43)
4D	33°38.5′	139°09.6′	1883	tilt	(2)	(>33)	0.67*	(>22)
4E	33°38.6′	139°09.6′	1883	tilt	(2)	(>30)	0.67*	(>20)
4F	33°38.6′	139°09.5′	1883	fell				
PC3-1	33°48.2′	140°38.3′	1867	1.5			0.81±0.03	
PC3-2	″	″	″	″			0.84±0.02	

Notes:

Depth: Water depth without correction for change in sound velocity.

PEN: Length of the probe in the sediment; "fell" means that the probe fell without penetration and "tilted" means that it did penetrate but not vertically.

N: Number of sensors that were used for calculation of "G".

G: Temperature gradient calculated by the least square method. The values with inequality sign (>) are the estimates as minimum values, whereas the ones linked by the dash indicate the range.

K: Thermal conductivity. Asterisk represents values measured at the nearby station.

Q: Heat flow as the product of G and K. Special signs mean the same as those used at "G".
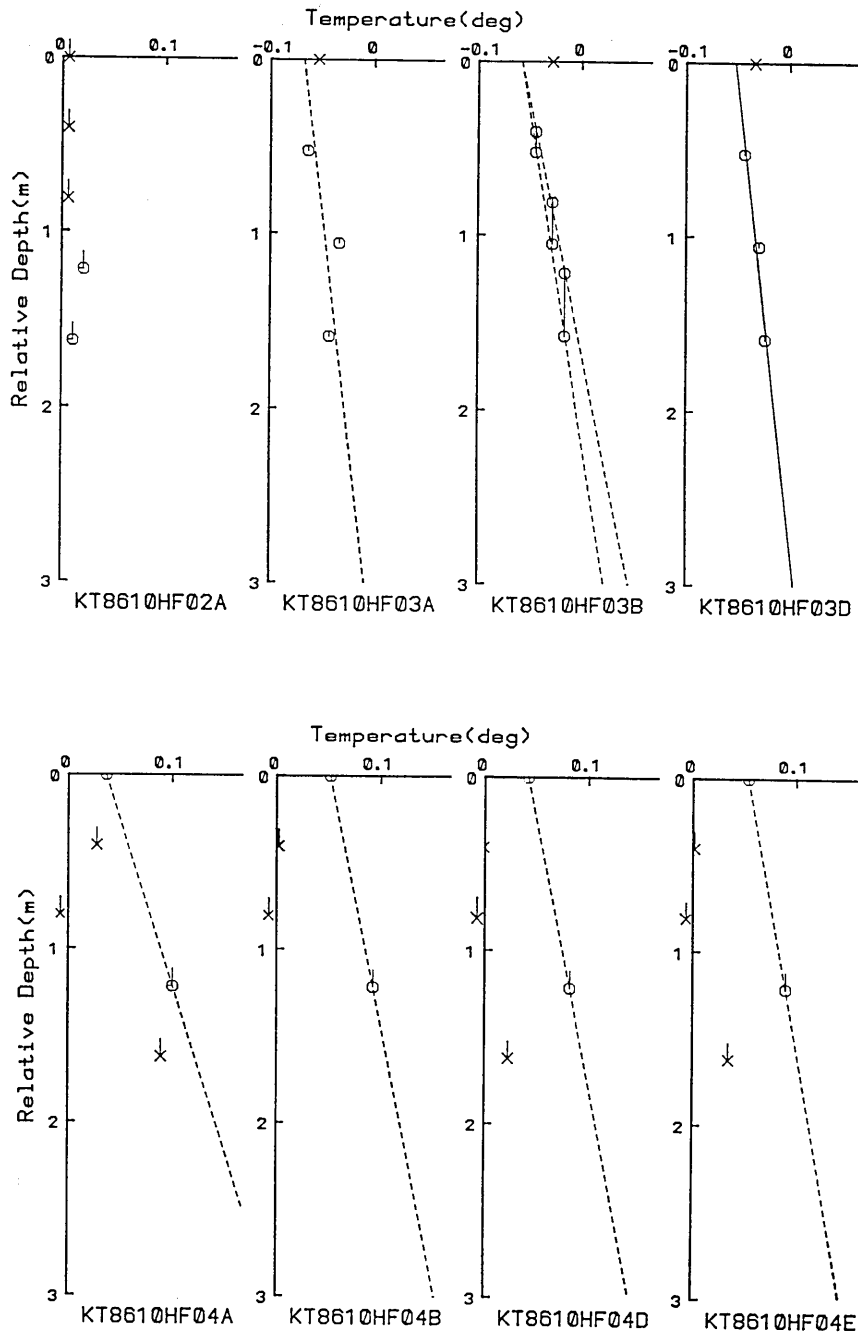
Fig. 21. Temperature versus depth profiles obtained at HF-2 to HF-4. Solid and dashed lines are obtained by the least square fit of the data. The x- mark data represent less reliable ones.

Thermal Conductivity(W/mK)
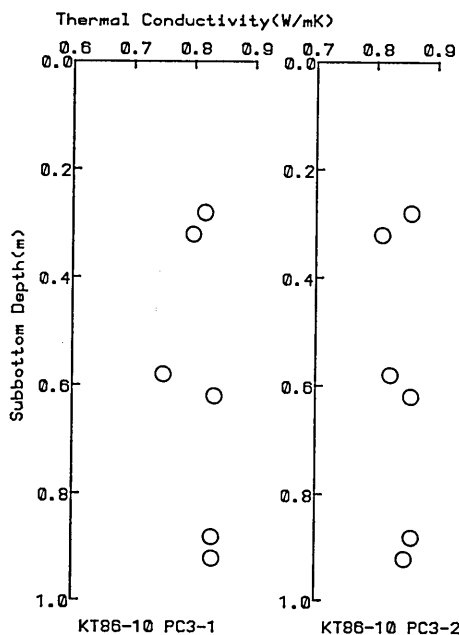
Fig. 22. Thermal conductivity versus depth profiles obtained from the samples taken by piston coring, P-3. PC3-1 and PC3-2 represent the first and second measurements respectively.

was corrected for the instrument tilt. The cross mark data represent less reliable ones due to the instability of the thermistor or ones which seem not to have penetrated in the sediment. The measured thermal conductivity values for the samples taken at P-3 are presented in Fig. 22.

HF-1 was located in the Hachijo Basin. The water depth was 1,290 m, and the topography was flat. However, probably due to the bottom current, the instrument tended to move apart from the bottom during the measurement of the reference temperature in the water. None of three trials was successful.

HF-2 and HF-4 were located in the western part of the Mikura Basin, where, through the surveys of the Maritime Safety Agency, Hydrographic Department and Geological Survey of Japan, acoustic anomalies were found (high by about 100 m) along the two normal faults trending north to south. Two anomalies were also detected on our cruise (Fig. 7a). HF-2 and HF-4 aimed at these two anomalies, but owing to the strong tidal flow the instrument hit the bottom about one kilometer apart from the anomalies. According to the core sample taken by a piston corer, the sediment was silty within several tens of centimeters from the bottom and sandy below that, which seems to have prevented the probe from penetrating well enough.

At HF-2, the probe appeared either not to have penetrated at all or to have stood largely tilted, judging from almost no temperature change (at most 0.02 deg) relative to the temperature of the sea water.

At HF-4 the temperature profiles in the sediment were not well determined partly because most of the thermistors were unstable and partly because no trial ended in vertical penetration. However, it was clear that the probe did penetrate, though tilted, and the minimum heat flow value was estimated using the record of stable sensors. The values obtained

were about 20 mW/m² or higher, which seems much lower than the previous values measured in the northern and eastern parts of the basin (75 mW/m² and 103 mW/m², respectively) as reported by WATANABE (1970). This variability of heat flow values might indicate that in the Mikura Basin hydrothermal circulation is occurring, although the density of measurement is too low. Moreover, as is recognized in Fig. 21, at HF-4 the topmost and the lowermost (fourth from the top) sensors showed significant increases in temperature relative to the bottom water temperature whereas the second and third sensors showed effectively no change. Unfortunately the upper two sensors were possibly unstable. However, if these features reflect the true temperature profiles, it may strongly suggest the existence of some thermal anomaly in the sediment near the surface.

HF-3 was located east of Kitakurose on the forearc slope (water depth : 1,500 m). The bottom condition was better and two of five trials were successful. The heat flow was low, around 17 mW/m². This value was lower than the value 86 mW/m² measured about 40 km south of HF-3 (VESEROV, 1975), and seems inconsistent with the idea of high heat flow in the forearc area by ANDERSON (1980) as already mentioned. This appears to show the localized nature of the thermal activity in the Izu-Ogasawara forearc region. Bottom water temperature change possibly affected the temperature in the mud, because the temperature profile of HF-3A was far from linear, and HF-3D profile is more or less convex upward (Fig. 21). The water depth around these stations was not deep enough, and a fairly large vertical temperature gradient existed in the water temperature near the bottom. Therefore, the reliability of the HF-3 data was low. However, there was no doubt that the value was significantly lower than other values in the forearc region. This variability should be clarified by further studies.

5. CTD observations

5-1. Principles and methods

It is expected that deep sea hydrothermal systems discharge hot fluid to cause local increases in bottom water temperature. WEISS *et al.* (1977) found a temperature anomaly up to 0.15°C in the Galapagos hydrothermal area by using the deep tow system of the Scripps Institution of Oceanography. Recently, SAKAI *et al.* (1987) towed a CTD system above the Loihi submarine volcano, Hawaii, and found several locations with temperature anomalies ranging from 0.025 to 0.080°C. Such bottom temperature

anomalies are regarded as conclusive evidence of active hydrothermal systems.

During the KT 86-10 Expedition, we conducted bottom CTD towing observations in the Mikura Basin area in order to search for temperature anomalies of bottom water. The method was almost the same as used by SAKAI *et al.* (1987) and is described below in detail. Our towing system consisted of a Neil Brown Mark III CTD equipped with 10-liter Niskin rosette multi samplers (General Oceanics, Model 1015-12-25) and a sonar pinger (Benthos, Model 2216) as shown in Fig. 23. The whole block diagram of the system including the deck unit is shown in Fig. 24. CTD signals (C: conductivity, T: temperature, and D: depth in decibars) were transmitted to the deck unit through the armored cable of the winch. The desk top computer (HP 9845B) calculated salinity (S) and displayed depth profiles of T and S in real time. At the same time the data were stored in the digital tape recorder for off-line jobs after the observation.

The CTD observation was performed in the following way. At first the towing fish was lowered just above the bottom, measuring ambient profiles of T and S. When the fish reached a depth several meters above the bottom, the computer was actuated to start the time-mode program which enabled it to display the changes of D, T and S against the elapsed time (every 0.8 sec) on the CRT. The distance between the system and the bottom, which was continuously monitored with the pinger, was kept at 2–5 m during the towing operations by raising or lowering the winch wire frequently. The towing speed was about one knot, and the towing usually continued 2–3 hours. When anomalous temperature data were recorded, one of the rosette samplers was triggered to close by transmitting the signal from the deck command. The collected waters was used for chemical analyses (see the next chapter).
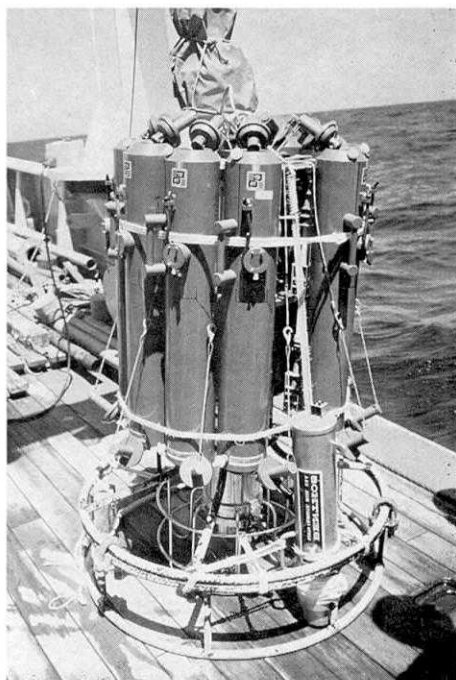
Fig. 23.   CTD with water sampling system.
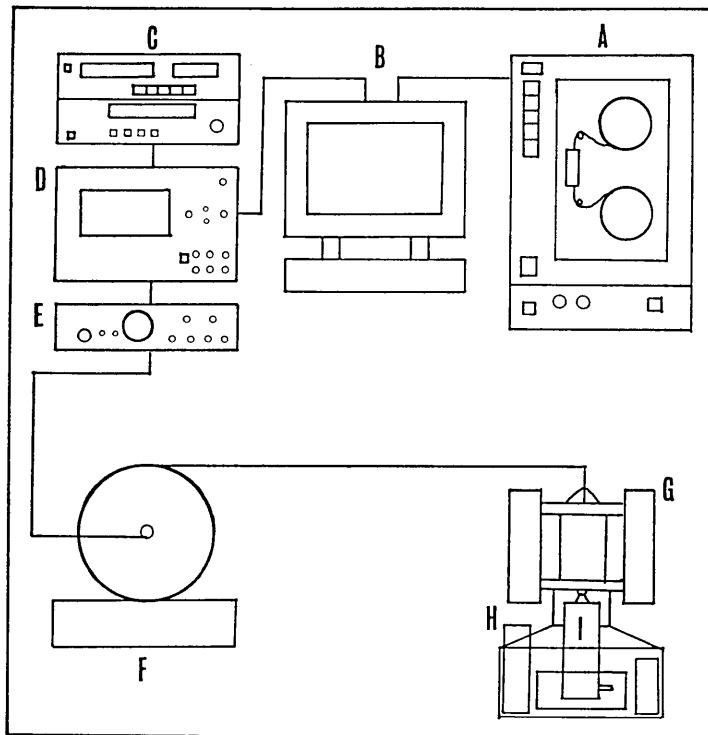
Fig. 24. Block diagram of CTD. A: digital tape recorder, B: computer (HP 9845B), C: video recorder and digital audio processor, D: CTD deck unit, E: deck command, F: winch, G: Rossete sampler, H: pinger, I: CTD.

5-2. Results and discussion

Fig. 25 shows the CTD record at station CTD-3-1-1, where the hydrothermal activity was suggested from the geological and geophysical observations. It could be seen that between 22:50 and 23:05 hours the temperature varied about 0.05°C with complicated zigzag patterns. Was this an indication of a hydrothermal plume?

In order to judge whether or not the temperature anomaly was really originated from the hydrotermal activity, the temperature record was corrected by using the ambient T-S relationship (WEISS *et al.* 1977). This correction is necessary because the bottom temperature anomalies could also be apparently arisen by local water mixings. We established the linear T-S relationship for the local water in the researched area as shown in Fig. 26. The least square method gave a linear function of $T = -7.436S + 259.4$. Therefore, the value of $T + 7.436S$ was invariant to the mixing processes of the local water.

Fig. 25. Temperature, salinity, and pressure records from an arbitrary data number
zero as the deep two CTD is towed 2–5 m above the bottom. T: temperature ('C),
S: salinity, P: pressure (db), T–S: the T–S function (T+XS), which is invariant
to mixing, with similar correction and smoothing.

In Fig. 25, this value was plotted as T–S. The T–S record showed a
straight trend with no anomaly, which means that T anomaly between
22 : 50 and 23 : 05 hours was the "false" (no hydrothermal) one. In fact,
the variation of S correlated inversely with that of T between 22 : 50 and
23 : 50 hours as shown in Fig. 25. Since the P (depth) record showed that
the CTD sensor was maintained at almost the same depth during the
towing, the changes of T and S were not due to the raising or lowering
of the CTD fish. Therefore, the temperature anomaly in Fig. 25 most
likely reflects a transient intrusive mixing of the shallower local water,
probably caused by bottom topographic features (Gamo and Horibe, 1984).

6. Chemical composition of the sea water

6-1. Sampling and analytical method
    It is known that hydrothermal fluids emanating from the submarine
hydrothermal system have distinctive chemical properties different from
that of normal sea water. Mixing with the hydrothermal fluids causes

Fig. 26. The T-S diagram shows that the entire array of water types represents a single water mass; the equation of correction is T=−7.436×S+259.357.

ambient sea water around the hydrothermal system to be enriched in various substances. By detecting such concentration anomalies we can find out submarine hydrothermal activities.

In order to search for evidence of hydrothermal activities in the Mikura Basin, we studied chemical compositions of sea water collected with the CTD rosette multi-sampling system (see chapter 5) during the KT 86-10 Cruise. As the hydrothermal indicators, methane, heavy metals and arsenic were chosen.

Samples were collected with a 10 *l*-Niskin type sampler (which has a stainless steel spring inside). Ten samplers were attached to the CTD towing system. At the towing site at Station CTD-3, seawater samples were collected during the CTD towing above a few meters from the bottom to search for water temperature anomalies, and at the reference site of Station CTD-4, we moved the CTD system vertically to collect samples at various depths to know the profile of each indicator.

Methane was analyzed with a FID gas chromatograph after extraction with helium (Gamo *et al.*, 1987). Heavy metals were analyzed by chelating resin preconcentration—atomic absorption spectrometry (AAS). Arsenic was analyzed by the Hydride-Generation Atomic Absorption Spectrometry coupled with Flow Injection Analysis (FIA-HGAAS) (Yamamoto *et al.*, 1985).

6-2. Results and discussion

Table 4 shows the observational data of *in situ* temperature (T), salinity (S), methane, heavy metals and arsenic. Data of depth, T, S were measured with the CTD sensors. Heavy metal concentrations in sea water near the Japan Trench and the Mariana Trough are also shown for comparisons.

All samples except for CTD-4-5 show low methane concentrations of less than 10 nl/kg. These values are almost the same as the methane background concentration for ordinary seawater 1,000–3,000 meters deep. Therefore, it can be said that no significant anomaly exists at Station

Table 4. Chemical composition of

Site	Sample No.	Depth (m)	T (°C)	S	CH_4 (nl/kg)	Cu (ng/l)	Pb (ng/l)
Towing Site	1	1,873	2.162	34.586	8.0	232	23
(CTD-3)	2	1,872	2.174	34.583	7.9	136	45
	3	1,867	2.138	34.589	5.6	158	24
	4	1,866	2.151	34.589	6.6	258	41
	5	1,866	2.182	34.581	5.4		
	7	1,865	2.161	34.584	7.8		
	8	1,866	2.184	34.582	4.6	127	15
	9	1,816	2.204	34.579	3.7		
	10	1,764	2.227	34.575	2.8	160	32
	11	1,665	2.368	34.461	3.5		
Reference Site	1	1,836			3.6	111	7
(CTD-4)	2	1,790			3.2		
	3	1,740			3.6	143	5
	4	1,642			3.4		
	5	1,343			10.8		
Japan Trench*						200	5
Mariana Trough**						250	

* Averege concentration of deep water at Japan Trench (3,000–6,000 m)
(Shitashima, unpublished data)
** Concentration of bottom water at Mariana Trough (3,500 m)
(Tsubota *et al.*, personal communication)

CTD-3.

Concentrations of arsenic were within the range of 1,350–1,450 ng/l in the Mikura Basin. As measured by Shitashima (unpublished data), they were 1,250–1,350 ng/l in the North Pacific and they are 1,400–1,600 ng/l above the Loihi (Hawaii) submarine volcano, where active hydrothermal systems were observed (SAKAI *et al.*, 1987). In the Mikura Basin, arsenic values were slightly higher than that in the North Pacific, but we could not decide whether these high values were due to hydrothermal activity or to the difference of arsenic distributions between the North Pacific and the Philippine Sea.

Generally speaking, Cu, Pb, Fe, Mn, Zn, Co, Ni and Cd concentrations at both the towing and reference sites in the Mikura Basin were higher than those in the Japan Trench. Some samples from the towing site had metal concentrations slightly higher than those collected from the reference site, and Cu, Fe and Zn concentrations at the towing site were as high as those in the Mariana Trough. Two samples from the towing site (1,867 meters and 1,872 meters depth) and one sample taken from the reference

sea water in the Mikura Basin

Fe (ng/l)	Mn (ng/l)	Zn (ng/l)	Co (ng/l)	Ni (ng/l)	Cd (ng/l)	Mo (ng/l)	V (ng/l)	As (ng/l)
2410	74	1280	1	814	132	13200	1920	1450
1150	74	553	(38)	(32500)	100	10100	1650	1380
2750	90	804	(36)	(39800)	126	11600	1760	1350
1780	68	1020	<1	897	130	11420	1840	1320
								1450
								1450
3220	99	620	<1	780	113	10700	1080	1380
								1380
508	75	1380	<1	545	119	11200	1720	1380
								1350
727	86	646	<1	549	118	12000	1780	1350
								1550
313	61	408	(28)	(30800)	105	10500	1660	1350
								1380
								1450
500	50	500	1	500	100	1100	1700	1350
1200	300	1000			200			

site (1,740 meters depth) showed that only Co and Ni concentrations were exceptionally high compared with other metal concentrations for these samples.

For most metals, especially for Pb, Fe and Zn, there may have been some contamination which could have originated from the water sampler or winch wire. But it was unlikely that such high values of Co and Ni for the three samples should be due to contamination or dissolution from sediments and minerals, because other metals (except Co and Ni) showed fairly low values. The origin of such high concentrations of Co and Ni is quite unclear. However, the existence of hydrothermal activity in the Mikura Basin may be one explanation that could account for these findings.

As mentioned above, no obvious evidence for a hydrothermal activity in the Mikura Basin was shown from the methane data. But slight anomalies were observed in heavy metal concentrations, which may be an indication of a hydrothermal activity. In order to confirm this, more detailed studies on spatial variations of methane, heavy metals and other indicators will be necessary in the future.

7. Discussion

The results obtained during the cruise were not enough to establish the tectonic development of the northern Izu-Ogasawara Arc. Preliminary interpretations on the topography, sediments, structures of the Mikura and Hachijo Basins will be briefly discussed in this chapter.

7-1. Topographic high

Topographic highs with anomalous seismic reflections both by 12 kHz and seismic profiler were discovered west of Inanbajima at water depths around 1,800 m. Deep sea photographs clearly showed that these topographic highs consist of angular boulders of volcanic rocks. These facts were reconfirmed by the collection of two pyroxene andesites collected by using submersible "Shinkai 2000" being similar to that cropping out at Mikurajima (FUJIOKA *et al.*, in press).

Seismic patterns across the topographic highs were quite similar to those obtained in the area where acoustic plumes were frequently observed. According to dive ♯252 by the submersible "Shinkai 2000" as well as the seismic data, each topographic high was several tens of meters high, several hundred meters wide and they stretched two or three miles from north-west to south-east (FUJIOKA *et al.*, in press). The topographic highs

should be called small andesitic knolls, because various sizes of blocky andesitic lava covered all the knolls.

Seismic profilers across the knolls clearly showed the existence of the faults, and beneath them there may exist hydrothermal ore deposits resulting from volcanic activity. TOKUYAMA *et al.* (1987) found a possible magma reservoir about 1.5 km beneath the knoll which supported the high possibility of finding ore deposits.

7-2. Development of the Mikura and Hachijo Basins

Three multichannel seismic profiler data were obtained during the cruise. The Mikura Basin was cut by many normal faults trending almost northwest to southeast, some of which cut the surface sediments. Therefore, these faults may be active. Three units of seismic stratigraphy of the basins were recognized according to Figs. 8a, 8b, 8c.

The uppermost layer was the Quaternary coarse sand consisting mostly of scoria and plankton tests. The age for the sediments less than 70 ky. was based on the nannofossil biostratigraphy of the piston core sediments. The second layer was well stratified and the folded strata possibly consisted of the volcanic edifices derived from adjacent volcanic islands or submarine volcanoes after the collapse on the rifting of the basins. The third layer was an acoustic basement which may be equivalent to the propyritic rocks of the Yugashima Group, because volcanic rocks exposed in the seven Izu Islands sometimes include gabbroic rocks and other kind of xenoliths similar to those of the Yugashima Group at Hachijojima, Miyakejima, Niijima and Oshima (ISSHIKI, 1959, 1980).

The development of the basin may be as described below.

At the initial stage of rifting normal faults formed the depression structures of the Mikura and Hachijo Basins stepwise scheme.

After the rifting, volcanic materials thickly masked the acoustic basement and the compressional stress field predominated to make folding, and later fissure eruption of lavas, andesitic in composition, pored out forming the small knolls parallel to the stress trajectory of σH maximum in this region (NAKAMURA *et al.*, 1981; FUJIOKA and SUGA, in press).

7-3. Temperature and chemistry of seawater

During CTD as well as heat flow measurements, small temperature anomalies were recognized as shown in Fig. 25. The scale of the temperature anomaly was 0.05°C compared to the temperature of the surrounding seawater. If this temperature anomaly reflected hydrothermal activity, the anomaly of sea water for instances He, CH_4 may

have been caused simultaneously.

By correcting the temperature anomaly (Fig. 25) using the relationship between temperature and salinity of the ambient seawater, it was suggested that the temperature anomalies measured during the cruise might have been caused by the mixing of two water masses. However, there is still room for the hydrothermal origin. During the ♯252 dive of "Shinkai 2000" Fe–Mn oxide coated andesitic rocks were recovered from the foot of the knoll (Fujioka *et al.*, in press). It is strongly expected that a precise CTD survey be made along the knoll as a future study for hydrothermal activity.

8. Summary

Results obtained during the KT 86-10 cruise of the Tansei-Maru, Ocean Research Institute, University of Tokyo (DELP 1986 cruise) are summarized below.

(1) Topographic highs with anomalous seismic patterns were found west of Inanbajima in the western part of the Mikura Basin. These are recognized to be a small mound consisting mostly of boulders of volcanic rocks.

(2) Sediments covering the Mikura and the Hachijo Basins are biogenic and volcanogenic in origin which reflect the drainage pattern of the area.

(3) Bottom dwelling organisms are so active that the surface sediments are well disturbed making small sandy mounds and holes for their nests.

(4) Terrestrial heat flow values across the Izu-Ogasawara arc-trench system show patterns similar to that across the ordinary arc-trench system.

(5) Temperature anomalies measured during the cruise may have originated by the mixing of the local shallower water ; however, there is still the possibility of finding hydrothermal activity.

(6) Geologic development of the basins was as given below. Normal faults relating to the rifting of northern Izu-Ogasawara backarc cut the acoustic basement followed by thick piles of volcanic edifices. Folding of the second unit and fissure eruption of two pyroxene andesite took place under the compressional stress field.

Acknowledgements

References

ANDERSON, R. N., 1980, 1980 Update of Heat Flow in the East and Southwest Asian Seas, in "The Tectonic and Geologic Evolution of Southwest Asian Seas and Islands", (D. E. Hayes, ed.), pp. 319-326, Geophys. Monograph 23, American Geophysical Union, Washington, D. C.

BULLARD, E. C., 1954, The flow of heat through the floor of the Atlantic Ocean, *Proc, R. Soc. London, Ser. A*, **222**, 408-429.

FUJIOKA, K., 1983, Where were the "kuroko deposits" formed, looking for the present day analogy, in E. Horikoshi ed. "Island Arcs, Marginal Seas, and Kuroko Deposits", Mining Geology Special Issue, The Society of mining Geologists of Japan, **11**, 55-68 (in Japanese with English abstract).

FUJIOKA, K., 1985, Submarine Topography around Sagami and Suruga Bays and their adjacent area, Jubil. Pub. Prof. J. Hosoi, 387-400 (in Japanese with English abstract).

FUJIOKA, K. and K. NAKAMURA, 1984MS, Tranist from northern Suruga (Box 5) to Sagami (Box 4), On Board Cruise Report KAIKO Project, Phase I, Leg 2.

FUJIOKA, K., T. ISHII, K. HAMURO, S. ARAMAKI, K. UTO, T. TANAKA and K. KONISHI, 1980, Rhyolites and quartz-diorites newly discovered from the sea bottom between the Oshima Island and the Niijima Island, Abstracts, The 87th Annual Meeting of the Geological Society of Japan, 152 (in Japanese).

FUJIOKA, K., T. FURUTA, T. IIYAMA, K. KOGA, K. NAKAMURA, Y. NAKAMURA, Y. OGAWA, A. TAKEUCHI, H. TANIGUCHI and M. WATANABE, 1984, Geology of the Boso Submarine escarpment, southeast of Tokyo-Preliminary report of the Tansei Maru Cruise KT83-20, *Bull. Earthq. Res. Inst., Univ. Tokyo*, **59**, 267-326 (in Japanese with English abstract).

FUJIOKA, K., T. FURUTA, G. KIMURA, K. KODAMA, K. KOGA, S. KURAMOTO. H. MATSUGI, T. SENO, A. TAKEUCHI, M. WATANABE and S. YAMAMOTO, 1986, Sediments and Rocks in and around the Palau and Yap Trenches, in Preliminary Report of the Hakuho Maru Cruise KH86-1, Y. Tomoda Ed., Ocean Res. Inst., University of Tokyo.

FUJIOKA, K., T. TANAKA, Y. IWABUCHI, K. KOGA and H. HOTTA, (in press), Submarine Andesite Knoll,—A deep-sea suvey by "Shinkai 2000" in the Mikura Basin, Tech. Rept. of JAMSTEC (in Japanese with English Abstract).

GAMO, T. and Y. HORIBE, 1984, Excess bottom Rn-222 profiles and their implications in the northwestern Pacific Ocean, *Earth Planet. Sci. Lett.*, **71**, 215-228.

GAMO, T., J. ISHIBASHI, H. SAKAI and B. TILBROOK, 1987, Methane anomalies in seawater

above the Loihi submarine summit area, Hawaii, *Geochim. Cosmochim. Acta.*, in press.

GARTNER, S., 1977, Calcareous nannofossil biostratigraphy and revised zonation of the Pleistcene, *Mar. Micropaleont.*, **2**, 1-25.

GEOLOGICAL SURVEY OF JAPAN, 1985, Investigation for evolution on the heavy metal sourse accompanied by the submarine hydrothermal activities (in Japanese).

VON HERZEN, R. P. and A. E. MAXWELL, 1959, The measurement of thermal conductivity of deep sea sediments by a needle-probe method, *J. Geophys. Res.* **64**, 1557-1563.

HONZA, E. and K. TAMAKI, 1985, Bonin Arc, in Ocean Basin and Margins: 7A, The Pacific Ocean, Nairn, A. E. M., Stehli, F. G., and Uyeda, S. Eds., Plenum Press, New York, 459-502.

HYDROGRAPHIC OFFICE MARITIME SAFETY AGENCY, 1980a, Bathymetric Chart, No. 6364, The Southwest of Miyake Shima.

HYDROGRAPHIC OFFICE MARITIME SAFETY AGENCY, 1980b, Bathymetric Chart, No. 6365, The Northeast of Hatizyo Shima.

HYDROGRAPHIC OFFICE MARITIME SAFETY AGENCY, 1982, Bathymetric Chart, No. 6313, Central Nippon.

ISHIBASHI, K., 1984, Plate motion in the southern Fossa Magna region —application to subduction of the Japan Sea—, *Chikyu*, **6**, 61-67 (in Japanese).

ISSHIKI, N., 1959, The Hachijo-jima, Quadrangle Series, scale 1:50,000, Geological Survey of Japan, pp. 58 (in Japanese with English Abstract).

ISSHIKI, N., 1980, Geology of the Mikurajima, Inambajima and Zenisu Districts, Quadrangle Series, scale 1:50,000, Geological Survey of Japan, pp. 35 (in Japanese with English Abstract, 3p).

MATSUBARA, Y., 1981, Heat flow measurements in the Bonin arc area, in "Geological investigation of the junction area of the Tohoku and Ogasawara arcs", (Miyazaki, T. and Honza, E., ed.), pp. 130-135, Cruise Report, No. 19, Geological Survey of Japan.

NAKAMURA, K., K. SHIMAZAKI and N. YONEKURA, 1984, Subduction, bending and education. Present and Quaternary tectonics of the northern border of the Philippine Sea plate, *Bull. Soc. geol. Frauce*, **26**, 221-243.

ONODERA, K. and K. MUKAI, 1976, Geomorphology of Izu Ogasawara arc and trench, in Izu-Ogasawara (Bonin) Arc and Trench Investigations, Inoue, E. Ed., Cruise Report No. 5, Geol. Surv. Japan, 25-28.

RATCLIFFE, E. H., 1960, The thermal conductivities of ocean sediments, *J. Geophys. Res.*, **65**, 1535-1541.

SAKAI, H., H. TSUBOTA, T. NAKAI, J. ISHIBASHI, T. AKAGI, T. GAMO, B. TILBROOK, G. IGARASHI, M. KODERA, K. SHITASHIMA, S. NAKAMURA, K. FUJIOKA, M. WATANABE, G. M. MCMURTRY, A. MALAHOFF and M. OZIMA, 1987, Hydrothermal activity on the summit of Loihi Seamount, Hawaii, *Geochem. J.*, **21**, 11-21.

SAKURAI. M. and M. OGAWA, 1982, Tectonic Movement in the Northern Part of the Nishi-Sitito Ridge, *Report of Hydrographic Office*, **17**, 1-12.

SCLATER, J. G., J. CROWE and R. N. ANDERSON, 1976, On the reliability of oceanic heat flow averages, *J. Geophys. Res.*, **81**, 2997-3006.

TAKEUCHI, A. and K. FUJIOKA, 1985, Submarine geomorphology along the Sagami and Suruga Troughs, *Jour. Geography*, **94**, 102-114 (in Japanese with English abstract).

TAMAKI, K., 1985, Two mode of back-arc spreading, *Geology*, **13**, 475-478.

TAMAKI, K., E. INOUE, M. YUASA, M. TANAHASHI and E. HONZA, 1981, On the possibility of Quaternary back-arc spreading activity in the Ogasawara arc, *The Earth Monthly*, **3**, 421-431 (in Japanese).

TOKUYAMA, H., E. NISHIYAMA, K. SHIMAMURA, K. SUZUKI and H. MIYATA, 1987, Bright Spot found from Mikura Basin—Implication of Magma Chamber, Programme and Abstracts, The Seismological Society of Japan, 1987, No, 1 (in Japanese).

UYEDA, S., 1983, Hydrothermal circulation in the ocean floor, Mariana trough, kuroko

and the mode of subduction, in E. Horikoshi ed. "Island Arcs, Marginal Seas, and Kuroko Deposits", Mining Geology Special Issue, The Society of Mining Geologists of Japan, 11, 37-53 (in Japanese with English abstract).

VACQUIER, V., S. UYEDA, M. YASUI, J. SCLATER, C. CORRY and T. WATANABE, 1966, Studies of the Thermal State of the Earth. The 19th. Paper: Heat Flow Measurements in the Northwestern Pacific, *Bull. Earthq. Res. Inst., Univ. Tokyo*, 44, 1519-1535.

VESEROV, O. V., G. D. YEREMIN, and G. SOINOV, 1975, Heat flow determination during the second complex oceanic expedition of the Sakhalin Complex Scientific Research Institute, in "Geophysical Researches of the Crust and Upper mantle structure in the Transition Zone from Asian Continent to the Pacific Ocean, 30", (I. K. Tyezov et al., eds.), 298-300, Akad. Nauk. Ussr. (in Russian).

WATANABE, T., D. EPP, S. UYEDA, M. LANGSETH and M. YASUI, 1970, Heat flow in the Philippine Sea, *Tectonophysics*, 10, 205-224.

WATANABE, T., M. LANGSETH and R. N. ANDERSON, 1977, Heat flow in back-arc basins of the Western Pacific, in "Island Arcs Deep Sea Trenches, and Back-arc Basins", (Talwani, M. and Pitman, W. C., eds.), pp. 137-167, Maurice Ewing Ser., Vol. 1, American Geophysical Union, Washington D. C.

WEISS, R. F,. P. LONSDALE, J. E. LUPTON, A. E. BAINBRIDGE and H. CRAIG, 1977, Hydrothermal plumes in the Galapagos Rift, *Nature*, 267, 600-603.

YAMAMOTO, M., M. YASUDA and Y. YAMAMOTO, 1985, Hydride-generation atomic absorption spectrometry coupled with flow injection analysis, *Anal. Chem.*, 57, 1382-1385.

YAMANO, M., 1985, Heat flow Studies of the Circum-Pacific subduction zones, (Doctor Thesis), pp. 15-16.

YAMAZAKI, T., 1985, Research Report, pp. 17-21, Geophysical Survey of Japan (in Japanese).

YAMAZAKI, T., 1986, High heat flow in the Ogasawara Rift, Programme and Abstracts, Seismol. Soc. Japan, 1986(1), 256 (in Japanese).

御蔵・八丈海盆における KT 86-10次航海報告

海洋研究所
　藤　岡　換太郎
　蒲　生　俊　敬
　蓮　本　浩　志
　石　橋　純一郎
　西　山　英一郎
　佐　柳　敬　造
　徳　山　英　一
　渡　辺　正　晴

地震研究所　　木　下　正　高
山形大学理学部　　崔　　　宰　豪

東北大学理学部
　布　施　圭　介
　田　中　裕一郎

日本大学文理学部　　古　家　和　英

千葉大学理学部
　宮　田　宏　紀
　鈴　木　敬　一

九州東海大学農学部　　嶋　村　　　清
広島大学総合科学部　　下　島　公　紀

　御蔵海盆と八丈海盆は伊豆・小笠原島弧一海溝系の火山フロントのすぐ背後に位置している．これらの海盆には海底熱水活動の存在が期待されている．東京大学海洋研究所の淡青丸による KT 86-10 次航海が1986年7月12日から21日の間行われ，この地域の地質学，地球物理学，及び地球化学的な調査がなされた．御蔵海盆の中央にある崗灘波島の西部から PDR と音波探査によって小さな地形的な高まりが発見された．この高まりは北北西一南南東の伸長方向を持ちその幅数100メートル，高さ数10メートルで2マイル程度連続する．これは，火山岩の巨礫の積み重なった小丘で，その深部には断層が発達している．この火山岩の大部分は両輝石安山岩であることが後の「しんかい2000」の潜水調査で確かめられた．周辺の海盆底は厚い火山源及び生物源物質によって埋立てられており，堆積物が底生生物によって著しく乱されている．これらの海盆の発達史は音波探査の記録から以下の通りまとめられる．まず伊豆・小笠原背弧のリフティングに関連した正断層群によって，この地域の基盤が切られ沈降した．ひきつづきこの基盤を厚い火山物質が覆った．次に，北北西一南南東方向の σhmax に平行な安山岩質溶岩の広域割れ目噴火を起こし，活断層と伴に小丘が形成され，この小丘を横切って CTD の観測が行われ小丘の近くで 0.05°C 程の温度異常が見つかった．小丘に沿って観測された温度と塩分濃度の関係は現在の熱水活動の存在に否定的である．しかし，マルチチャンネル音波探査の結果は御蔵海盆の深さ約 1.5 km のところにマグマ溜りの存在を示している．島弧を横切る方向の地殻熱流量の値の分布が火山フロントで高く，背弧でもやや高いこと，断層による陥没及び活断層の存在，深海カメラや潜水艇で熱水性堆積物らしいものが撮影されていること，潜水艇のマニピュレータで得られた安山岩に Fe-Mn に富む堆積物が付着していたことなどは海盆に熱水活動の存在することを支持しているが，この海域のもっと丹精なる調査が将来必要である．